

Supervising 3D Talking Head Avatars with Analysis-by-Audio-Synthesis

Radek Daněček

Carolin Schmitt

Senya Polikovsky

Michael J. Black

Max Planck Institute for Intelligent Systems

{radek.danecek, cschmitt, senya, black}@tuebingen.mpg.de

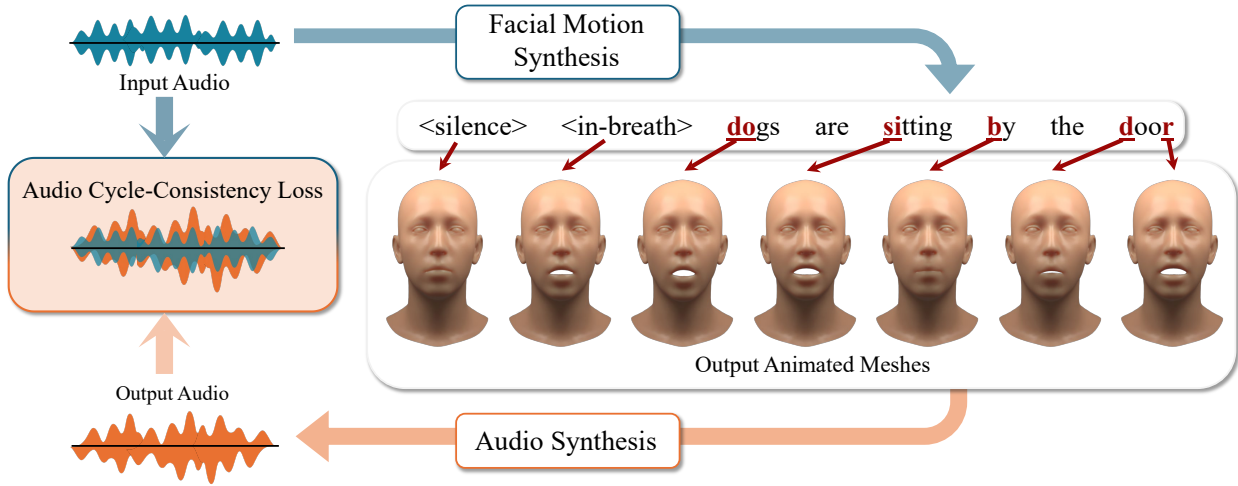


Figure 1. THUNDER introduces a new paradigm for stochastic generation of 3D talking head avatars from speech with accurate lip articulation and diverse facial expressions. Given an input audio, a 3D animation is generated. The animation is then fed into an audio synthesis (mesh-to-speech) model, which generates an output audio representation. The input and output audio representations are compared, creating a novel audio-consistency supervision loop, which we coin as *analysis-by-audio-synthesis*.

Abstract

In order to be widely applicable, speech-driven 3D head avatars must articulate their lips in accordance with speech, while also conveying the appropriate emotions with dynamically changing facial expressions. The key problem is that deterministic models produce high-quality lip-sync but without rich expressions, whereas stochastic models generate diverse expressions but with lower lip-sync quality. To get the best of both, we seek a stochastic model with accurate lip-sync. To that end, we develop a new approach based on the following observation: if a method generates realistic 3D lip motions, it should be possible to infer the spoken audio from the lip motion. The inferred speech should match the original input audio, and erroneous predictions create a novel supervision signal for training 3D talking head avatars with accurate lip-sync. To demonstrate this effect, we propose THUNDER (Talking Heads Under Neural Differentiable Elocution Reconstruction), a 3D talking head avatar framework that introduces a novel supervision mechanism via differentiable sound production. First, we train a novel mesh-to-speech model that regresses audio from facial animation. Then, we incorporate this model into a diffusion-based talk-

ing avatar framework. During training, the mesh-to-speech model takes the generated animation and produces a sound that is compared to the input speech, creating a differentiable analysis-by-audio-synthesis supervision loop. Our extensive qualitative and quantitative experiments demonstrate that THUNDER significantly improves the quality of the lip-sync of talking head avatars while still allowing for generation of diverse, high-quality, expressive facial animations.

1. Introduction

Animating 3D faces from speech has many applications. Examples include the entertainment industry (games and movies), applications in AR/VR/XR (virtual telepresence), e-commerce and perhaps future embodied digital assistants. In order to be widely applicable, the 3D head avatars must, however, appear and act believably and feel alive. While the methods to animate 3D avatars from speech have come a long way in recent years, there is still a considerable realism gap between real humans and 3D avatars.

Seminal approaches such as VOCA [15] or Karras et al. [43], and others [17, 25, 57] are deterministic regres-

sors, that predict 3D vertices from the input audio. Despite achieving good lip-sync, these methods produce facial animations without emotion [15, 25] or that are unnaturally static [17, 57]. This is in part due to the lack of large-scale and expression-rich training data and in part because a deterministic regressor cannot accurately produce animations of facial motions that only weakly correlate with the audio (such as eyebrow motion, eyeblinks, etc.). Hence, in order to generate animations that appear lively and believable, a good 3D speech-driven system must model the problem in a non-deterministic manner so that it can capture the many-to-many mapping between speech and facial animation.

Consequently, recent methods model the problem of 3D speech-driven animation stochastically using relatively small datasets of high-quality 3D scans [65, 69, 78, 86]; the small training size limits diversity and expressiveness. Other methods leverage lower-quality pseudo ground-truth (GT) extracted from larger-scale video datasets [70, 93]. In pursuing diversity, however, stochastic methods vary the lip motions in ways that deviate from the audio signal.

The fundamental issue is that lip motions, for the same audio, vary with expression. We seek a method that generates diverse expressions but is faithful to the audio. So we ask the question: “What does it mean to be faithful to the audio?” This leads us to our key observation; that is, we seek 3D lip motions that *actually reproduce the input audio*. We formalize this notion with a **new form of supervision** for 3D speech-driven avatars using a novel **mesh-to-speech** model; see Fig. 1. Inspired by recent silent-video-to-speech (SVTS) methods [11, 44, 45], we propose, to our knowledge, the first mesh-to-speech model. Our mesh-to-speech model regresses the speech audio (or a representation thereof) solely from the animated 3D face. In other words, every generated animation now also produces a sound. Our rationale is simple: the more similar the produced sound is to the input speech, the more plausible the animation. Furthermore, failure to produce the correct sound should provide a good supervision signal.

Our system consists of two stages. In the first stage, we train the mesh-to-speech model to regress audio from facial motion. In the second stage, we train a diffusion model to output 3D facial animation from speech. In this stage, we utilize the frozen mesh-to-speech model. The generated facial animation is fed into the mesh-to-speech model, effectively reproducing the spoken audio. This generated audio (or representation thereof) is then compared to the input audio, creating a self-supervised training loop; this is illustrated in Fig. 1. We refer to this as *analysis-by-audio-synthesis*. Our experiments show that leveraging the mesh-to-speech model results in much better lip-sync quality, while still enabling stochastic production of expressive speech-driven animation.

In summary, our contributions are: (1) A novel **mesh-to-speech** model that regresses sound from 3D facial animations. (2) A new form of **cross-modal audio-based self-**

supervision via comparison of the representations of the input speech and the animation-produced output speech. (3) A 3D speech-driven animation method based on diffusion, capable of generating a variety of facial expressions while maintaining accurate lip-sync. The code and models will be made publicly available at <https://thunder.is.tue.mpg.de/>.

2. Related work

2.1. Speech-driven 3D animation

The field of speech-driven 3D facial animation has made significant progress in the last two decades [7, 12, 21, 22, 72, 87]. Here we focus on the recent deep-learning based line of work [2, 3, 15, 17, 23–25, 43, 53, 54, 57–59, 65, 69, 70, 73, 78, 86, 90, 93, 94].

Deterministic neural methods. Karras et al. [43] were the first to utilize deep learning by training a temporal convolutional network (TCN) to predict 3D face vertices. VOCA [15] employs a pre-trained automatic speech recognition (ASR) network to regress face vertex offsets from audio, achieving good lip-sync for multiple speaking styles. Many follow-up methods use a similar paradigm [2, 17, 23–25, 29, 31, 53, 54, 56, 57, 79, 88].

Stochastic neural methods. The first model to approach the problem stochastically was MeshTalk [65]. MeshTalk makes use of a pretrained discretized facial motion prior along with an explicit supervision mechanism that supports generation of motions that only have a weak correlation with the audio (eyebrow motion, etc.). CodeTalker [86] upgrades the FaceFormer architecture by predicting codebook classes of a pretrained VQ-VAE. Both MeshTalk and CodeTalker employ autoregressive prediction and one can therefore sample the distribution of the next token to generate variety.

Thanks to the tremendous success of Diffusion Models in the image domain [34, 67] they are now widely used for 3D human body animation [8, 74], as well as speech-driven animation [69, 70, 78, 93]. The diffusion methods also employ transformer-based audio feature extractors [4, 36] to condition the denoiser. FaceDiffuser [69] employs a GRU-based denoiser, 3DiFACE [78] uses a TCN-based denoiser, and DiffPoseTalk [70], Media2Face [93] and FaceTalk [3] employ a transformer decoder architecture [81] passing the audio condition to the denoiser via cross-attention.

Controlling the output animation. The task of controlling or editing the output animation is of great utility in production as manually editing animations is a laborious process. Many methods use a simple one-hot encoding of training subjects, which is mapped to a “style embedding” with a learnable layer. This embedding conditions the decoder to match the speaking style of the corresponding training subject [15, 25, 79, 86]. This paradigm has been extended to control the emotion and emotion intensity [17, 57]. Diff-

PoseTalk [70] uses contrastive learning to produce a style vector from a reference animation, lifting the subject-ID conditioning limitation. Media2Face [93] employs CLIP features [62], which can be extracted from an image, or text prompts to condition the denoising process. 3DiFACE [78] demonstrates that the output of a diffusion model can be guided by a sparse set of keyframes. In this paper, instead of focusing on controlling the animation, we present a general method to improve lip-sync quality, which can be used in conjunction with the above control mechanisms.

Datasets. Most methods [15, 25, 43, 79, 86] have made use of high quality 3D scans synchronized with audio, such VOCASET [15], BIWI [26] or Multiface [85]. While these datasets are of high quality, they are expensive to acquire and hence are limited in number of subjects, and richness of facial expressions. The dataset design is often a limiting factor, as the samples are usually sentences taken out of context and hence the subjects do not express themselves in the most natural ways. As a consequence, even the stochastic methods that leverage these datasets [65, 69, 86], suffer from lack of natural diversity of expressions.

Thanks to the significant improvement of in-the-wild face reconstruction systems [16, 28, 64, 92, 95] that can now be utilized off-the-shelf, recent methods have turned to using pseudo-ground-truth (pGT) reconstructions from videos [17, 57, 70, 93]. While the pGT does not reach the quality of 3D scans, video datasets are numerous, allowing more data to be acquired, which benefits data-hungry stochastic models.

2.2. Silent-video-to-speech (SVTS)

To the best of our knowledge, the prediction of voice from a sequence of 3D facial shapes has never been explored. However, recent years have seen tremendous progress on the task of speech audio prediction from silent videos. Early methods [14, 35, 44, 52, 55, 80, 83, 89] focus on small in-the-lab datasets with predefined scripts and limited number of speakers (GRID [13], TCD-TIMIT [32]) or script-unconstrained but single-speaker models [60].

STVS [19] was the first method to produce intelligible audio on large-scale in-the-wild datasets such as LRS2 and LRS3 [1] by regressing spectrograms from mouth crops. The spectrograms are converted to the final waveform with a pretrained vocoder [11]. Follow-up methods improve the prediction quality [45] by adding a surrogate ASR loss or predicting features from an ASR model [11].

The most recent architectures are based on diffusion, producing audio often indistinguishable from real speech [10, 91]. These, however, are not suitable for a self-supervised reconstruction loop, due to the iterative nature of diffusion models.

Hence, thanks to its simple, yet efficient feed-forward design and a relatively straightforward architecture and training, we base our mesh-to-speech model on Choi et al. [11].

2.3. Audio cycle consistency

Cycle consistency losses on audio have been applied before, for tasks like voice conversion [40–42] and disentangled representation learning [9, 39]. Many different self-supervised audio learning methods exist (see survey [49]). However, cross-modal cycle consistency between audio and 3D facial motion has, to our knowledge, never been proposed.

3. Preliminaries

3.1. Face model

THUNDER uses the FLAME face model [48], which is a statistical 3D morphable model (3DMM). FLAME provides a compact representation of facial shapes and expressions and is defined as a function:

$$M(\beta, \theta, \psi) \rightarrow (\mathbf{V}, \mathbf{F}), \quad (1)$$

where the inputs are shape coefficients $\beta \in \mathbb{R}^{|\beta|}$, expression coefficients $\psi \in \mathbb{R}^{|\psi|}$ and rotation vectors for $k = 4$ joints $\theta \in \mathbb{R}^{3k+3}$. FLAME outputs a 3D mesh with vertices $\mathbf{V} \in \mathbb{R}^{n_v \times 3}$ and triangles $\mathbf{F} \in \mathbb{R}^{n_f \times 3}$. Since we do not focus on head movement, we only use the jaw joint rotation θ_{jaw} . For brevity, we refer to the expression coefficients and jaw rotation as expression parameters $\mathbf{x} = [\psi | \theta_{jaw}]$.

3.2. Speech feature extraction

Following previous work on speech-driven facial animation [17, 25, 79, 86, 93] we use Wav2Vec2.0 [4] as our audio feature extractor. It consists of a temporal convolution network (TCN) that extracts audio features at 50Hz and a transformer encoder that processes these features. Similarly to previous methods, we resample the TCN feature to 25Hz and feed it to the transformer to obtain the final speech feature. Formally, we define this as: $\mathcal{A}(\mathbf{w}) \rightarrow \mathbf{a}^{1:T}$, where \mathcal{A} denotes the Wav2Vec 2.0 network, \mathbf{w} is the input waveform, and $\mathbf{a}^{1:T} \in \mathbb{R}^{T \times d_s}$, with T denoting the number of frames at 25Hz and $d_s = 768$ is the feature dimension.

3.3. Speaker Embedding

A speaker embedding is a numerical representation of a speaker's unique vocal characteristics encoded into a vector. This vector captures features such as tone, pitch, speaking style, and other vocal attributes, enabling the differentiation and recognition of individual speakers. Among other applications, speaker embeddings are used in the latest SVTS models [11, 19, 45]. Following Choi et al. [11], we leverage an off-the-shelf speaker embedding extractor [37]. We define the extractor as: $\mathcal{S}(\mathbf{w}) \rightarrow \mathbf{s}$, with \mathcal{S} and \mathbf{s} denoting embedding extractor and the embedding vector, respectively.

3.4. Speech Units

The term speech units refers to discrete linguistic units identified through a self-supervised learning process. Like

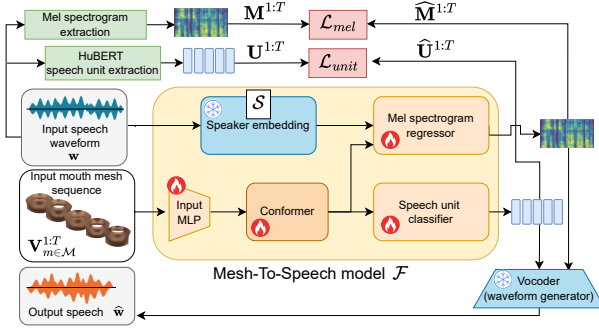


Figure 2. **Mesh-to-speech architecture.** It takes a sequence of mouth shapes as input, along with a speaker embedding feature, to produce the output speech units and spectrograms. These are used to compute a loss (top) and to produce the reconstructed audio (bottom) using a pretrained vocoder.

Choi et al. [11], we leverage speech units predicted by a pretrained HuBERT [36] model and its associated feature clustering model. First, features are extracted and subsequently clustered into n_U units. We define speech units as one-hot class vectors $\mathbf{U} \in [c_1, c_2, \dots, c_{n_U}]$ where only one of $c_i, i = 1 \dots c_{n_U}$ is 1 and the rest are 0. Speech units are predicted at 50Hz.

4. Method

THUNDER is trained in two stages. First, a mesh-to-speech network is trained to regress audio from facial motion. Second, a diffusion model is trained to output 3D facial animation. The output animation is then fed to the frozen mesh-to-speech model producing output audio representations. This allows us to design a loss between the input and output representations, which we utilize in training the talking head system.

4.1. Mesh-To-Speech

Regressing audio from 3D facial motion has, to our knowledge, not been done before. To narrow down the architecture search space, we take inspiration from a recent SVTS model, namely Choi et al. [11].

Architecture. The architecture consists of an input feature encoder, a conformer sequence encoder and two prediction heads, a speech unit classifier, and a mel spectrogram regressor. These two outputs contain enough information that a pretrained off-the-shelf vocoder [11] can turn them into output audio. Since the input is not a video, but a 3D animation, we replace the original lip video ResNet encoder that Choi et al. [11] use with an MLP that takes 3D lip vertex coordinates as the input. We keep the rest of the architecture the same. The mesh-to-speech architecture is depicted in Fig. 2 and

can be written

$$\mathcal{F}(\mathbf{V}_{m \in \mathcal{M}}^{1:T}, \mathbf{s}) \rightarrow (\widehat{\mathbf{M}}^{1:T}, \widehat{\mathbf{U}}^{1:T}), \quad (2)$$

where $\mathcal{F}(\cdot)$ denotes the mesh-to-speech network, \mathcal{M} is a subset of mouth vertices. $\widehat{\mathbf{M}}^{1:T}, \widehat{\mathbf{U}}^{1:T}$ denote the output sequence of mel spectrograms and speech units. Finally, $\widehat{\mathbf{M}}^{1:T}$ and $\widehat{\mathbf{U}}^{1:T}$ can be passed to an off-the-shelf vocoder to generate the output waveform $\widehat{\mathbf{w}}$.

Supervision. We follow the same supervision scheme as Choi et al. [11]. The loss consists of two terms. The first term is an L1 loss between the input and output mel spectrograms:

$$\mathcal{L}_{mel} = \|\mathbf{M}^{1:T} - \widehat{\mathbf{M}}^{1:T}\|_1. \quad (3)$$

The second term is cross entropy between the predicted speech unit classification vectors and the GT speech units:

$$\mathcal{L}_{unit} = \frac{1}{T} \sum_{t=1}^T \sum_{c=1}^{n_U} \mathbf{U}_c^t \log p(\widehat{\mathbf{U}}_c^t), \quad (4)$$

with weights $w_{mel} = 10$ and $w_{unit} = 1$. The final loss is:

$$\mathcal{L}_{m2s} = w_{mel} \mathcal{L}_{mel} + w_{unit} \mathcal{L}_{unit}. \quad (5)$$

4.2. Speech-Driven Facial Animation Diffusion

Architecture. The core of THUNDER consists of a denoiser in the form of a transformer decoder [81]. Similar to other contemporary 3D animation methods (e.g. Zhao et al. [93] and Sun et al. [70]), THUNDER processes a noisy sequence of expression parameters $\tilde{\mathbf{x}}_{(d)}^{1:T}$, where d represents the diffusion timestep. These parameters serve as the *query* inputs to the transformer. The *keys* and *values* for the transformer are comprised of the input audio features $\mathbf{a}^{1:T}$ and a diffusion step embedding $\mathcal{T}(d)$, concatenated along the temporal dimension. The function \mathcal{T} is defined as a sinusoidal timestep function similar to Ho et al. [34]. We do not incorporate additional animation-controlling conditions (such as style vectors [15, 25, 86], emotion vectors [17, 57] or CLIP embeddings [93]) as this is not the goal of this work. However, the design can easily be augmented with additional input conditions. All inputs are projected into the transformer’s feature dimension, $f = 128$, using dedicated learnable affine layers. Positional encoding within the transformer’s self-attention utilizes the ALiBi mechanism [61]. The cross-attention layers use a diagonal binary mask to facilitate the attention mechanism, and no additional positional encoding. The model predicts the reconstructed expression parameters $\widehat{\mathbf{x}}_{(0)}^{1:T}$. The transformation can be formally described by the following equation:

$$\mathcal{D}(\tilde{\mathbf{x}}_{(d)}^{1:T}, d, \mathbf{a}^{1:T}) \rightarrow \widehat{\mathbf{x}}_{(0)}^{1:T}. \quad (6)$$

Here, $d \in \{1, \dots, D\}$ indicates the diffusion timestep, and $\widehat{\mathbf{x}}_{(0)}^{1:T}$ is the denoised prediction. Unlike some methods that

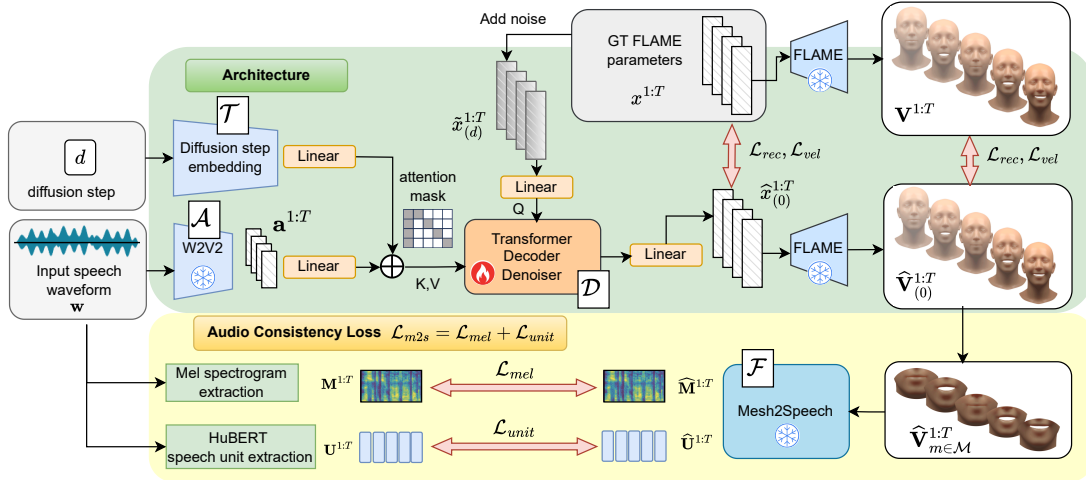


Figure 3. **Diffusion architecture.** The upper part of the figure (green) depicts the architecture of the diffusion model and the lower part (yellow) illustrates the application of the audio consistency loss. Gray boxes indicate the input to the system. Trainable components are highlighted in orange and frozen ones in blue.

predict noise, this model directly predicts the fully denoised space, which is used to compute the 3D mesh sequence: $M(\beta = 0, \hat{x}_{(0)}^{1:T}) \rightarrow \hat{V}_{(0)}^{1:T}$. This approach allows the model to define losses directly on the final 3D mesh space, crucial for leveraging mesh-to-speech. See Fig. 3 for an overview. **Training.** During training, a diffusion step d is sampled and $\tilde{x}_{(d)}^{1:T}$ is computed from the clean expression parameters $x^{1:T}$ using a noise schedule that blends the original data with Gaussian noise based on predefined α values:

$$\tilde{x}_{(d)}^{1:T} = \sqrt{\alpha_d} x^{1:T} + \sqrt{1 - \alpha_d} \cdot \epsilon, \quad \epsilon \sim \mathcal{N}(\mu, \Sigma), \quad (7)$$

where α_d represents the proportion of the original signal's variance preserved at diffusion timestep d , and ϵ is drawn from a Gaussian distribution with predefined μ and Σ . This approach incrementally corrupts the clean parameters, enabling the model to learn to denoise varying levels of noise. The model is supervised with several loss terms - reconstruction and velocity losses in expression space and 3D vertex space, and also the mesh-to-speech loss (Eq. (5)). The reconstruction loss is given as:

$$\begin{aligned} \mathcal{L}_{rec} = & \text{MSE}(\mathbf{V}^{1:T}, \hat{\mathbf{V}}_{(0)}^{1:T}) + \text{MSE}(\psi^{1:T}, \hat{\psi}_{(0)}^{1:T}) + \\ & \text{MSE}(\theta_{jaw}^{1:T}, \hat{\theta}_{jaw(0)}^{1:T}). \end{aligned}$$

The velocity loss is also an MSE error but computed on the velocities of the individual components:

$$\begin{aligned} \mathcal{L}_{vel} = & \text{MSE}(v(\mathbf{V}^{1:T}), v(\hat{\mathbf{V}}_{(0)}^{1:T})) + \text{MSE}(v(\psi^{1:T}), v(\hat{\psi}_{(0)}^{1:T})) + \\ & \text{MSE}(v(\theta_{jaw}^{1:T}), v(\hat{\theta}_{jaw(0)}^{1:T})), \end{aligned}$$

where v computes the velocity of any input sequence $\mathbf{u}^{1:T}$

$v(\mathbf{u}^{1:T}) = \mathbf{u}^{2:T} - \mathbf{u}^{1:T-1}$. The final loss is given as:

$$\mathcal{L}_{total} = w_{m2s} \mathcal{L}_{m2s} + \mathcal{L}_{rec} + \mathcal{L}_{vel}, \quad (8)$$

with $w_{m2s} = 1$. The model is trained using classifier-free guidance [33]. The audio condition is randomly dropped and replaced with a learnable vector with 20% probability.

Inference. At inference time, we initialize the first step by sampling the Gaussian noise: $\hat{x}_{(D)} \sim \mathcal{N}(\mu, \Sigma)$. We then proceed to denoise for D diffusion steps. In each step, we first employ the denoiser $\mathcal{D}(\tilde{x}_{(d)}, d, \mathbf{a}^{1:T})$ to obtain $\hat{x}_{(0)}^{1:T}$. Then, we compute $\tilde{x}_{(d-1)}$ by adding the expected amount of noise back to obtain $\tilde{x}_{(d-1)}$. Since THUNDER is trained with classifier-free guidance, it is possible to trade-off fidelity of the lip-sync for increased diversity by combining $s_a \mathcal{D}(\tilde{x}_{(d)}, d, \mathbf{a}^{1:T}) + (1 - s_a) \mathcal{D}(\tilde{x}_{(d)}, d, \emptyset)$ during the denoising process. However, we find our results are diverse enough without this and so we effectively set $s_a = 1$.

5. Experiments

5.1. Datasets

The selection of datasets for THUNDER is challenging. On the one hand, 4D scan datasets such as VOCASET [15] provide good reconstructions but are too small to train generative models. On the other hand, in order to have a high-enough quality geometry from which speech can be predicted, we cannot rely on in-the-wild datasets, as reconstruction artifacts decrease the quality of the GT and hence our mesh-to-speech and talking head models.

Hence, we use a collection of public in-the-wild captured video datasets commonly used for lip-reading, namely TCD-TIMIT [32], RAVDESS [50] and GRID [13], totaling 117

subjects, uttering 42140 short sentences, totaling 3535816 frames at 25FPS (over 39 hours). These datasets provide clear imagery without in-the-wild complexity and can be reconstructed by off-the-shelf methods to a satisfactory degree. Following EMOTE [17], we utilize the publicly available INFERNO framework [18], which contains a SOTA face reconstruction system [16, 28, 95]. We split each of the datasets by subjects, 70% for training and 15% each for validation and testing.

5.2. Mesh-To-Speech

Implementation details. We initialize the conformer and prediction heads with pretrained weights from Choi et al. [11]. The input MLP is trained from scratch. We train the model with the Adam optimizer [46] for 20 epochs and select the checkpoint with the lowest validation loss (reached within 5 epochs). The training batch size is 16 and the input sequence is trimmed to 125 frames.

Quantitative comparison. Since the mesh-to-speech model is the first of its kind, we compare mesh-to-speech to a recent silent-video-to-speech model [11] which we finetune on the videos from our training dataset for fair comparison. Note that FLAME does not model the teeth or tongue, which makes the mesh-to-speech task arguably harder than video-to-speech. Teeth and tongue, which may be visible on video, are critical for production of certain phonemes, such as labiodentals (/f/, /v/), or alveolar phonemes (/s/, /z/, /t/, /d/, /l/) [47]. Consequently, we do not expect mesh-to-speech to match the performance of a video-based method.

Table 1 reports the standard video-to-speech metrics, namely Short-Time Objective Intelligibility [71], Extended STOI [38] to measure the intelligibility of the generated samples, Perceptual Evaluation of Speech Quality (PESQ) [66] (narrow and wide band) to measure the perceptual quality, and Word Error Rate (WER), which we measure with the SOTA ASR network Whisper[63]. As expected, mesh-to-speech is not as accurate as video-to-speech, but the performance is comparable, suggesting that there is sufficient audio signal in the 3D to be useful for our downstream task. Note that mesh-to-speech is, however, more accurate than Choi et al.’s original (but not the fine-tuned) model. We experiment with the following input spaces for mesh-to-speech - selection of mouth vertices $\mathbf{V}_{m \in \mathcal{M}}$ (*mouth2s*), all vertices \mathbf{V} (*exp2s*), and FLAME expression parameters \mathbf{x} (*exp2s*) and report the results in Tab. 1. Remarkably, the model which takes global expression vectors, performs slightly better than the selection of mouth vertices $\mathbf{V}_{m \in \mathcal{M}}$. Despite that, we choose *mouth2s* to be our final model, as it results in better lip-sync supervision (discussed in Sec. 5.3 and Tab. 2). Please refer to the Sup. Video for audible comparison and Sec. A.1 in Sup. Mat. for further discussion on performance.

Modality	Model:	STOI \uparrow	ESTOI \uparrow	PESQ-WB \uparrow	PESQ-NB \uparrow	WER \downarrow
Mesh-to-speech	<i>exp2speech</i> \mathbf{x}	0.502	0.273	1.257	1.468	0.648
	<i>face2speech</i> \mathbf{V}	0.458	0.203	1.225	1.437	0.953
	<i>mouth2speech</i> $\mathbf{V}_{m \in \mathcal{M}}$	0.506	0.272	1.246	1.457	0.678
Video-to-speech	Choi et al. (finetuned)	0.555	0.348	1.281	1.511	0.437
	Choi et al. (orig)	0.376	0.141	1.126	1.313	1.011

Table 1. **Quantitative comparison** of video-to-speech and forms of mesh-to-speech (*mouth2speech*, *face2speech* and *exp2speech*).

5.3. Speech-Driven Facial Animation

Implementation details. THUNDER is trained using the Adam optimizer for 260 epochs with batch size 48, sequence length of 70 frames, and $D = 1000$ diffusion steps with a linear noise schedule. The transformer has 8 layers with 4 heads and feature dim $f = 128$.

Baselines. We compare THUNDER to other speech-driven avatar methods that are also trained on pGT and which output 3DMM parameters (as opposed to vertices). We reimplemented and trained several SOTA methods, namely FlameFormer (an adaptation of FaceFormer [25]), Media2Face [93] and DiffPoseTalk [70] (see Sup. Mat. for details). Unless stated otherwise, we keep the pretrained Wav2Vec weights frozen. Models that finetune Wav2Vec are denoted with a suffix -T (T for trainable).

Evaluation protocol. For each test audio sequence, we generate $S=32$ outputs. Each of these is initialized with a different random noise in the case of diffusion models, or randomly sampled subject-id condition in case of FlameFormer. Then we compute the following evaluation metrics, averaged out across the S outputs (unless stated otherwise).

Lip Vertex Error. Following [65, 70, 86] we report LVE, which calculates the maximum L2 error of all lip vertices for each frame and then computes the average over all frames.

Dynamic Time Warping. We also report the DTW proposed by Thambiraja et al. [79]. First, distances between the midpoints of lower and upper lips are calculated for both the predictions and GT. The two resulting time series are then used to compute the DTW distance.

Lip Correlation Coefficients. We argue that the above metrics are not comprehensive enough as LVE only operates over a sparse set of lip vertices and does not model the temporal aspect very well as each frame is handled separately and DTW only models the lower-upper lip distance. Specifically, we compute Pearson and Concordance correlation coefficients for every vertex coordinate in the mouth-region and average the coefficients. PCC and CCC are commonly used metrics for comparing time series.

Face dynamic deviation. An important aspect of facial animation, is the expressiveness of the upper face vertices. Following CodeTalker [86], we report Face Dynamics Deviation (FDD), which measures the differences between the temporal standard deviation of the pGT and the predicted vertices, averaged over a set of vertices. We report upper-FDD

Experiment	Model	LVE ↓	L-CCC ↑	L-PCC ↑	DTW ↓	S-DIV-U ↑	T-DIV-U ↑	S-DIV-L ↓	T-DIV-L ↑	T-FDD-U ↓	T-FDD-L ↓
THUNDER and mesh-to-speech input space	THUNDER w/o m2s	0.879	0.359	0.568	0.329	0.0419	0.044	0.21	0.254	0.0118	0.0932
	THUNDER w/ face2s	0.804	0.411	0.633	0.285	0.0297	0.0409	0.128	0.237	0.0117	0.0827
	THUNDER w/ exp2s	0.83	0.362	0.63	0.296	0.0404	0.0398	0.176	0.228	0.0125	0.0939
	THUNDER w/ mouth2s	0.802	0.426	0.639	0.29	0.0322	0.04	0.134	0.241	0.0122	0.0806
THUNDER and trainable audio enc.	THUNDER-T w/o m2s	0.723	0.428	0.623	0.266	0.02	0.0411	0.0656	0.216	0.0118	0.0811
	THUNDER-T w/ mouth2s	0.709	0.445	0.66	0.256	0.021	0.039	0.0669	0.202	0.0118	0.0788
Mesh-to-speech with other methods and additional input conditions	FlameFormer*	0.809	0.368	0.57	0.291	0.0271	0.0372	0.132	0.239	0.0117	0.0909
	FlameFormer* w/ m2s	0.794	0.411	0.614	0.265	0.0263	0.0393	0.111	0.219	0.0107	0.0715
	Media2Face*	0.96	0.308	0.531	0.363	0.0163	0.0459	0.108	0.256	0.0105	0.0899
	Media2Face* w/ m2s	0.815	0.428	0.609	0.282	0.0128	0.0586	0.0371	0.233	0.0154	0.083
	DiffPoseTalk*	0.68	0.464	0.612	0.267	0.025	0.0379	0.117	0.223	0.0101	0.0776
	DiffPoseTalk* w/ m2s	0.651	0.469	0.653	0.268	0.0172	0.0377	0.0604	0.204	0.0117	0.0813

Table 2. **Quantitative evaluation** of THUNDER, other models and ablations. (1) **Mesh-to-speech input space.** All of the mesh-to-speech variants are applicable. THUNDER with *mouth2s* results in the best lip-sync performance (LVE, L-CCC, L-PCC), which is why we select it as the final THUNDER model. *exp2s* is applicable, too as its scores best on DTW and has good diversity (S-DIV-U), while *face2s* scores the worst on diversity (S-DIV-U, T-DIV-U). (2) **Trainable audio encoder.** THUNDER-T results in improved lip-sync metrics (LVE, L-CCC, L-PCC and DTW), but at the slight expense of diversity of outputs (mainly upper face diversity S-DIV-U and T-DIV-U) compared to THUNDER which does not train the audio encoder. (3) **Mesh-To-Speech applied to other methods.** The application of mesh-to-speech to our reimplementations of Media2Face* (diffusion with image conditioning), DiffPoseTalk* (diffusion with style feature conditioning) and FlameFormer (deterministic with subject ID conditioning) improves lip-sync metrics at slight expense of expression diversity. Please note that DiffPoseTalk* and Media2Face* (both with and without mesh-to-speech) have a considerably lower diversity than THUNDER. This happens due to the additional conditioning inputs which narrow down the output distribution space. This also manifests itself with better lip-sync performance.

(FDD-U) and lip-FDD (FDD-L).

Sample diversity. One of the most important aspects of stochastic models is that they generate diverse animations for the same input. Remarkably, previous work has not analyzed this aspect [69, 70, 93]. We compute standard deviations of vertex distances between the pGT and the predictions for the same input at frame t . Formally, given a tensor of per-vertex L2 distances $\mathbf{D} \in \mathbb{R}^{N \times S \times T \times n_v}$, with N being the size of the test dataset and $S = 32$ is the number of sampled outputs per input. We compute the standard deviation along the sample dimension S . Other dimensions are subsequently averaged. We measure sample diversity for the upper face region (S-Div-U) and the lip region (S-Div-L).

Temporal diversity metric. We also report the temporal diversity, where the standard deviation is computed over the temporal dimension of $\mathbf{D} \in \mathbb{R}^{N \times S \times T \times n_v}$ (and averaged across the rest). Again, we calculate the diversity for both lip (T-Div-L) and upper face regions (T-Div-U).

5.3.1. Quantitative evaluation

Tab. 2 reports the computed metrics computed on the test set for THUNDER, baselines and ablations.

Ablation study. We ablate our design decisions. (1) The input space for the mesh-to-speech loss, (2) the trainability of the audio encoder (Tab. 2), and (3) the weight of the mesh-to-speech loss (see Sec. A.2.2 in Sup. Mat. and video).

Mesh-to-speech loss with other methods. Tab. 2 shows that mesh-to-speech is applicable to other methods. We reimplement three methods that incorporate additional conditioning mechanisms and train them with and without our mesh-to-speech loss. Our new loss improves performance on

the lip-sync metrics. For visual results, refer to Sup. Video.

Comparison to additional methods. Tab. 7 in Sup. Mat. we also include a comparison of THUNDER and other (original) implementations recent methods.

Disentanglement effect. To test whether mesh-to-speech helps preserve the effect of good lip-sync in the presence of other *editing conditions*, we additionally run our reimplementations of Media2Face with conditioning inputs extracted from emotional images. See Sec. A.2.1 in Sup. Mat.

Other datasets. To verify, whether THUNDER is dataset-agnostic, we also trained and tested the method on TFHP. We report the results in Sec. A.2.4 in Sup. Mat..

Perceptual study. We conduct a perceptual study in which we evaluate THUNDER and the effect of mesh-to-speech. Specifically, we compare to the deterministic FlameFormer, THUNDER with and without mesh-to-speech, and p-GT. The participants are shown two videos side-by-side and asked to rate animations on a five-point Likert scale (strong/weak preference for A or B or indifferent). We ask the participants to rate three aspects of the animation: lip-sync quality, dynamism, and realism. Fig. 4 reports the results for THUNDER and Fig. 5 for THUNDER-T. For the remaining results of the study and further discussion, see Sec. A.2.3 in Sup. Mat.

5.3.2. Qualitative evaluation

We demonstrate the superiority of our method qualitatively. Fig. 6 shows the comparison of our method with the baselines for selected utterances. Additional qualitative evaluation, can be found in the supplemental video and PDF.

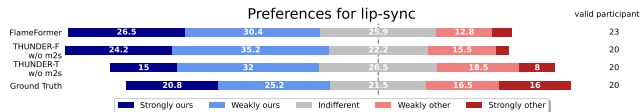


Figure 4. Perceptual study of THUNDER. We compare THUNDER-F with methods having both a trainable audio encoder (THUNDER-T w/o m2s) and frozen encoders (FlameFormer-F, THUNDER-F w/o m2s), and GT. The participants prefer THUNDER-F’s lip-sync over that of other models, but does not quite reach the fidelity of GT. Remarkably, the participants also have slight preference for THUNDER-F over GT, which suggests that the application of mesh-to-speech helps THUNDER saturate the quality of GT.

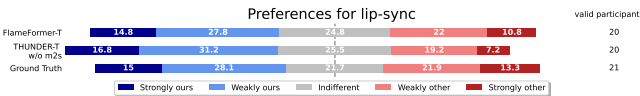


Figure 5. Perceptual study of THUNDER-T. We compare THUNDER-T with methods having both a trainable audio encoders (FlameFormer-T, THUNDER-T w/o m2s) and GT. Models with trainable backbones, achieve good lip-sync than their frozen counterparts, but THUNDER-T is still preferred over the other models.

5.4. Limitations

THUNDER has the following limitations. The absence of teeth and tongue inherently creates ambiguity, making it more difficult to produce high quality audio compared to silent video-to-speech. Further, pseudo-GT is not a perfect reconstruction but has occasional artifacts or inaccuracies. Also, our current mesh-to-speech architecture is fully deterministic and hence is not completely capable of capturing the prediction ambiguities. All of these may result in suboptimal effects of the audio cycle-consistency loss. However, regardless of these shortcomings, our experiments demonstrate the benefits of our method. Employing a large-scale dataset of high quality 3D scans, a face model that models teeth and tongue, and upgrade mesh-to-speech to a stochastic model are likely to boost the benefits of the mesh-to-speech loss. Finally, the inference process of the diffusion model is currently computationally intensive. Future work should address this by employing more efficient solvers such as DPM++ [51].

6. Conclusion

In this paper, we introduced THUNDER, a 3D speech-driven avatar generation system with a novel paradigm of supervision via analysis-by-audio-synthesis. THUNDER has two key components. First, drawing inspiration from silent video-to-speech methods, we define a new mesh-to-speech task

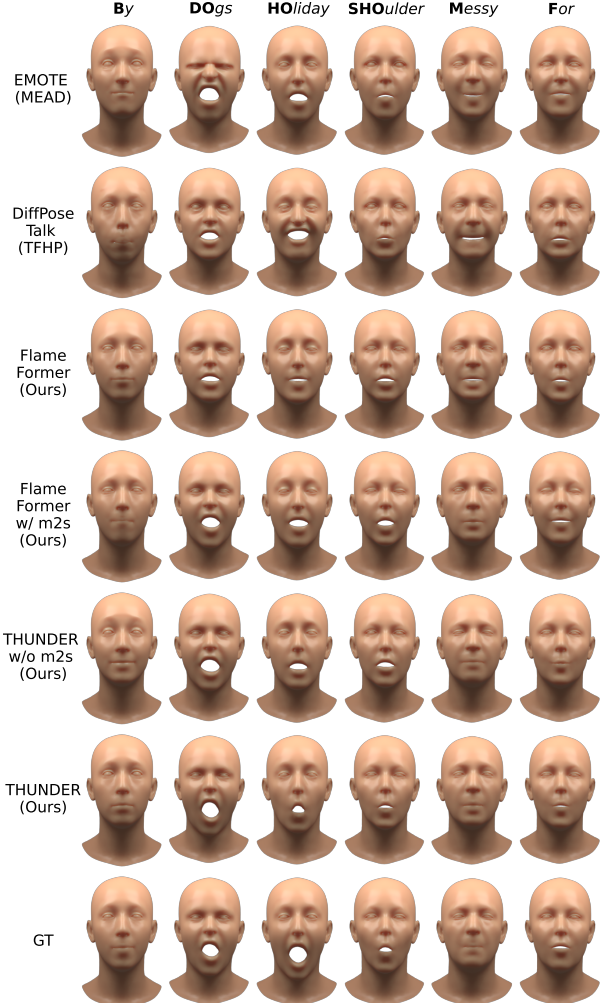


Figure 6. Qualitative comparison. This figure shows the comparison between baselines, our model and GT for selected utterances. The method’s training dataset is listed in parentheses below.

and train a model that regresses speech from facial animation. Second, we incorporated mesh-to-speech into a diffusion-based 3D speech-driven avatar system, creating the first-of-its-kind audio-based self-supervision loop that helps ensure that the produced lip animation is plausible for the spoken audio. Our extensive quantitative, perceptual, and qualitative experiments demonstrate that THUNDER achieves a significant improvement in lip animation quality for diffusion-based 3D speech-driven avatars while still producing a diverse set of facial animations. Furthermore, we have demonstrated that the application of our mesh-to-speech loss improves the lip-sync quality of other talking head avatar systems. Finally, we believe that our novel audio-based self-supervision paradigm can impact other applications of 3D head avatars, such as video-based reconstruction, automatic postprocessing of 3D facial animation, or as a quality measure of talking head avatars.

References

[1] Triantafyllos Afouras, Joon Son Chung, and Andrew Zisserman. LRS3-TED: a large-scale dataset for visual speech recognition. *CoRR*, abs/1809.00496, 2018. 3, 7

[2] Shivangi Aneja, Artem Sevastopolsky, Tobias Kirschstein, Justus Thies, Angela Dai, and Matthias Nießner. GaussianSpeech: Audio-driven gaussian avatars, 2024. 2

[3] Shivangi Aneja, Justus Thies, Angela Dai, and Matthias Nießner. Facetalk: Audio-driven motion diffusion for neural parametric head models. In *Proceedings of the IEEE/CVF Conference on Computer Vision and Pattern Recognition*, pages 21263–21273, 2024. 2

[4] Alexei Baevski, Yuhao Zhou, Abdelrahman Mohamed, and Michael Auli. wav2vec 2.0: A framework for self-supervised learning of speech representations. *Advances in Neural Information Processing Systems*, 33:12449–12460, 2020. 2, 3

[5] Volker Blanz, Sami Romdhani, and Thomas Vetter. Face identification across different poses and illuminations with a 3D morphable model. pages 202–207, 2002. 5

[6] Volker Blanz, Curzio Basso, Tomaso A. Poggio, and Thomas Vetter. Reanimating faces in images and video. *Computer Graphics Forum (Proc. EUROGRAPHICS)*, 22(3):641–650, 2003. 5

[7] Yong Cao, Wen C. Tien, Petros Faloutsos, and Frédéric Pighin. Expressive speech-driven facial animation. *ACM Trans. Graph.*, 24(4):1283–1302, 2005. 2

[8] Xin Chen, Biao Jiang, Wen Liu, Zilong Huang, Bin Fu, Tao Chen, and Gang Yu. Executing your commands via motion diffusion in latent space. In *Proceedings of the IEEE/CVF Conference on Computer Vision and Pattern Recognition*, pages 18000–18010, 2023. 2

[9] Kiran Chhatre, Radek Daněček, Nikos Athanasiou, Giorgio Becherini, Christopher Peters, Michael J. Black, and Timo Bolkart. AMUSE: Emotional speech-driven 3D body animation via disentangled latent diffusion. In *Proceedings of the IEEE/CVF Conference on Computer Vision and Pattern Recognition (CVPR)*, pages 1942–1953, 2024. 3

[10] Jeongsoo Choi, Joanna Hong, and Yong Man Ro. Diffv2s: Diffusion-based video-to-speech synthesis with vision-guided speaker embedding. In *IEEE/CVF International Conference on Computer Vision, ICCV 2023, Paris, France, October 1-6, 2023*, pages 7778–7787. IEEE, 2023. 3

[11] Jeongsoo Choi, Minsu Kim, and Yong Man Ro. Intelligible lip-to-speech synthesis with speech units. In *24th Annual Conference of the International Speech Communication Association, Interspeech 2023, Dublin, Ireland, August 20-24, 2023*, pages 4349–4353. ISCA, 2023. 2, 3, 4, 6

[12] Michael M. Cohen, Rashid Clark, and Dominic W. Marsaro. Animated speech: research progress and applications. In *Auditory-Visual Speech Processing, AVSP 2001, Aalborg, Denmark, September 7-9, 2001*, page 200. ISCA, 2001. 2

[13] Martin Cooke, Jon Barker, Stuart Cunningham, and Xu Shao. The grid audio-visual speech corpus, 2006. 3, 5

[14] Thomas Le Cornu and Ben Milner. Reconstructing intelligible audio speech from visual speech features. In *16th Annual Conference of the International Speech Communication Association, INTERSPEECH 2015, Dresden, Germany, September 6-10, 2015*, pages 3355–3359. ISCA, 2015. 3

[15] Daniel Cudeiro, Timo Bolkart, Cassidy Laidlaw, Anurag Ranjan, and Michael J. Black. Capture, learning, and synthesis of 3d speaking styles. In *IEEE Conference on Computer Vision and Pattern Recognition, CVPR 2019, Long Beach, CA, USA, June 16-20, 2019*, pages 10101–10111. Computer Vision Foundation / IEEE, 2019. 1, 2, 3, 4, 5

[16] Radek Daněček, Michael J. Black, and Timo Bolkart. EMOCA: emotion driven monocular face capture and animation. In *IEEE/CVF Conference on Computer Vision and Pattern Recognition, CVPR 2022, New Orleans, LA, USA, June 18-24, 2022*, pages 20279–20290. IEEE, 2022. 3, 6, 5, 7

[17] Radek Daněček, Kiran Chhatre, Shashank Tripathi, Yandong Wen, Michael Black, and Timo Bolkart. Emotional speech-driven animation with content-emotion disentanglement. In *SIGGRAPH Asia 2023 Conference Papers*, New York, NY, USA, 2023. Association for Computing Machinery. 1, 2, 3, 4, 6, 5, 7

[18] Radek Daněček. INFERNO: Set the world on fire with FLAME. <https://github.com/radekd91/inferno>, 2023. 6, 7

[19] Rodrigo Schobburg Carrillo de Mira, Alexandros Haliassos, Stavros Petridis, Björn W. Schuller, and Maja Pantic. SVTS: scalable video-to-speech synthesis. In *23rd Annual Conference of the International Speech Communication Association, Interspeech 2022, Incheon, Korea, September 18-22, 2022*, pages 1836–1840. ISCA, 2022. 3

[20] Yu Deng, Jiaolong Yang, Sicheng Xu, Dong Chen, Yunde Jia, and Xin Tong. Accurate 3d face reconstruction with weakly-supervised learning: From single image to image set. In *IEEE Conference on Computer Vision and Pattern Recognition Workshops, CVPR Workshops 2019, Long Beach, CA, USA, June 16-20, 2019*, pages 285–295. Computer Vision Foundation / IEEE, 2019. 5

[21] Pif Edwards, Chris Landreth, Eugene Fiume, and Karan Singh. Jali: An animator-centric viseme model for expressive lip synchronization. *ACM Trans. Graph.*, 35(4), 2016. 2

[22] Pif Edwards, Chris Landreth, Mateusz Popławski, Robert Malinowski, Sarah Watling, Eugene Fiume, and Karan Singh. Jali-driven expressive facial animation and multilingual speech in cyberpunk 2077. In *ACM SIGGRAPH 2020 Talks*, New York, NY, USA, 2020. Association for Computing Machinery. 2

[23] Han EunGi, Oh Hyun-Bin, Kim Sung-Bin, Corentin Nivelet Etcheberry, Suekyeong Nam, Janghoon Joo, and Tae-Hyun Oh. Enhancing speech-driven 3d facial animation with audio-visual guidance from lip reading expert. *CoRR*, abs/2407.01034, 2024. 2

[24] Xiangyu Fan, Jiaqi Li, Zhiqian Lin, Weiye Xiao, and Lei Yang. Unitalker: Scaling up audio-driven 3d facial animation through A unified model. In *Computer Vision - ECCV 2024 - 18th European Conference, Milan, Italy, September 29-October 4, 2024, Proceedings, Part XLI*, pages 204–221. Springer, 2024.

[25] Yingruo Fan, Zhaojiang Lin, Jun Saito, Wenping Wang, and Taku Komura. Faceformer: Speech-driven 3d facial animation

with transformers. In *IEEE/CVF Conference on Computer Vision and Pattern Recognition, CVPR 2022, New Orleans, LA, USA, June 18-24, 2022*, pages 18749–18758. IEEE, 2022. 1, 2, 3, 4, 6, 7

[26] G. Fanelli, J. Gall, H. Romsdorfer, T. Weise, and L. Van Gool. A 3-d audio-visual corpus of affective communication. *IEEE Transactions on Multimedia*, 12(6):591 – 598, 2010. 3

[27] Yao Feng, Haiwen Feng, Michael J. Black, and Timo Bolkart. Learning an animatable detailed 3D face model from in-the-wild images. 40(4):88:1–88:13, 2021. 5, 7

[28] Panagiotis P. Filntisis, George Retsinas, Foivos Paraperas-Papantoniou, Athanasios Katsamanis, Anastasios Roussos, and Petros Maragos. Visual speech-aware perceptual 3d facial expression reconstruction from videos, 2022. 3, 6, 2, 4, 5, 7

[29] Hui Fu, Zeqing Wang, Ke Gong, Keze Wang, Tianshui Chen, Haojie Li, Haifeng Zeng, and Wenxiong Kang. Mimic: Speaking style disentanglement for speech-driven 3d facial animation. In *Thirty-Eighth AAAI Conference on Artificial Intelligence, AAAI 2024, Thirty-Sixth Conference on Innovative Applications of Artificial Intelligence, IAAI 2024, Fourteenth Symposium on Educational Advances in Artificial Intelligence, EAAI 2024, February 20-27, 2024, Vancouver, Canada*, pages 1770–1777. AAAI Press, 2024. 2

[30] Rohit Girdhar, Alaaeldin El-Nouby, Zhuang Liu, Mannat Singh, Kalyan Vasudev Alwala, Armand Joulin, and Ishan Misra. Imagebind one embedding space to bind them all. In *IEEE/CVF Conference on Computer Vision and Pattern Recognition, CVPR 2023, Vancouver, BC, Canada, June 17-24, 2023*, pages 15180–15190. IEEE, 2023. 5

[31] Kazi Injamamul Haque and Zerrin Yumak. Facehubert: Text-less speech-driven e(x)pressive 3d facial animation synthesis using self-supervised speech representation learning. In *INTERNATIONAL CONFERENCE ON MULTIMODAL INTERACTION (ICMI '23)*, New York, NY, USA, 2023. ACM. 2

[32] Naomi Harte and Eoin Gillen. TCD-TIMIT: an audio-visual corpus of continuous speech. *IEEE Trans. Multim.*, 17(5): 603–615, 2015. 3, 5

[33] Jonathan Ho and Tim Salimans. Classifier-free diffusion guidance. *CoRR*, abs/2207.12598, 2022. 5

[34] Jonathan Ho, Ajay Jain, and Pieter Abbeel. Denoising diffusion probabilistic models. In *Advances in Neural Information Processing Systems 33: Annual Conference on Neural Information Processing Systems 2020, NeurIPS 2020, December 6-12, 2020, virtual*, 2020. 2, 4

[35] Joanna Hong, Minsu Kim, Se Jin Park, and Yong Man Ro. Speech reconstruction with reminiscent sound via visual voice memory. *IEEE ACM Trans. Audio Speech Lang. Process.*, 29: 3654–3667, 2021. 3

[36] Wei-Ning Hsu, Benjamin Bolte, Yao-Hung Hubert Tsai, Kushal Lakhota, Ruslan Salakhutdinov, and Abdelrahman Mohamed. Hubert: Self-supervised speech representation learning by masked prediction of hidden units. *IEEE/ACM Transactions on Audio, Speech, and Language Processing*, 29:3451–3460, 2021. 2, 4

[37] Corentin Jemine. Real-time voice cloning. <https://github.com/CorentinJ/Real-Time-Voice-Cloning>, 2023. 3

[38] Jesper Jensen and Cees H. Taal. An algorithm for predicting the intelligibility of speech masked by modulated noise maskers. *IEEE ACM Trans. Audio Speech Lang. Process.*, 24(11):2009–2022, 2016. 6

[39] Xinya Ji, Hang Zhou, Kaisiyuan Wang, Wayne Wu, Chen Change Loy, Xun Cao, and Feng Xu. Audio-driven emotional video portraits. In *IEEE Conference on Computer Vision and Pattern Recognition, CVPR 2021, virtual, June 19-25, 2021*, pages 14080–14089. Computer Vision Foundation / IEEE, 2021. 3

[40] Takuhiro Kaneko and Hirokazu Kameoka. Parallel-data-free voice conversion using cycle-consistent adversarial networks. *CoRR*, abs/1711.11293, 2017. 3

[41] Takuhiro Kaneko, Hirokazu Kameoka, Kou Tanaka, and Nobukatsu Hojo. Cyclegan-vc2: Improved cyclegan-based non-parallel voice conversion. In *IEEE International Conference on Acoustics, Speech and Signal Processing, ICASSP 2019, Brighton, United Kingdom, May 12-17, 2019*, pages 6820–6824. IEEE, 2019.

[42] Takuhiro Kaneko, Hirokazu Kameoka, Kou Tanaka, and Nobukatsu Hojo. Cyclegan-vc3: Examining and improving cyclegan-vcs for mel-spectrogram conversion. In *21st Annual Conference of the International Speech Communication Association, Interspeech 2020, Virtual Event, Shanghai, China, October 25-29, 2020*, pages 2017–2021. ISCA, 2020. 3

[43] Tero Karras, Timo Aila, Samuli Laine, Antti Herva, and Jaakko Lehtinen. Audio-driven facial animation by joint end-to-end learning of pose and emotion. *ACM Transactions on Graphics (TOG)*, 36(4):1–12, 2017. 1, 2, 3

[44] Minsu Kim, Joanna Hong, and Yong Man Ro. Lip to speech synthesis with visual context attentional GAN. In *Advances in Neural Information Processing Systems 34: Annual Conference on Neural Information Processing Systems 2021, NeurIPS 2021, December 6-14, 2021, virtual*, pages 2758–2770, 2021. 2, 3

[45] Minsu Kim, Joanna Hong, and Yong Man Ro. Lip-to-speech synthesis in the wild with multi-task learning. In *ICASSP 2023-2023 IEEE International Conference on Acoustics, Speech and Signal Processing (ICASSP)*, pages 1–5. IEEE, 2023. 2, 3

[46] Diederik P. Kingma and Jimmy Ba. Adam: A method for stochastic optimization. In *3rd International Conference on Learning Representations, ICLR 2015, San Diego, CA, USA, May 7-9, 2015, Conference Track Proceedings*, 2015. 6

[47] Peter Ladefoged and Keith Johnson. A course in phonetics (sixth edition). 2011. 6

[48] Tianye Li, Timo Bolkart, Michael. J. Black, Hao Li, and Javier Romero. Learning a model of facial shape and expression from 4D scans. 36(6):194:1–194:17, 2017. 3, 6

[49] Shuo Liu, Adria Mallol-Ragolta, Emilia Parada-Cabaleiro, Kun Qian, Xin Jing, Alexander Kathan, Bin Hu, and Björn W. Schuller. Audio self-supervised learning: A survey. *Patterns*, 3(12):100616, 2022. 3

[50] Steven R. Livingstone and Frank A. Russo. The Ryerson Audio-Visual Database of Emotional Speech and Song (RAVDESS), 2018. 5

[51] Cheng Lu, Yuhao Zhou, Fan Bao, Jianfei Chen, Chongxuan Li, and Jun Zhu. Dpm-solver++: Fast solver for

guided sampling of diffusion probabilistic models. *CoRR*, abs/2211.01095, 2022. 8

[52] Daniel Michelsanti, Olga Slizovskaia, Gloria Haro, Emilia Gómez, Zheng-Hua Tan, and Jesper Jensen. Vocoder-based speech synthesis from silent videos. In *21st Annual Conference of the International Speech Communication Association, Interspeech 2020, Virtual Event, Shanghai, China, October 25-29, 2020*, pages 3530–3534. ISCA, 2020. 3

[53] Federico Nocentini, Thomas Besnier, Claudio Ferrari, Sylvain Arguillère, Stefano Berretti, and Mohamed Daoudi. Scantalk: 3d talking heads from unregistered scans. In *Computer Vision - ECCV 2024 - 18th European Conference, Milan, Italy, September 29-October 4, 2024, Proceedings, Part XXIX*, pages 19–36. Springer, 2024. 2

[54] Federico Nocentini, Claudio Ferrari, and Stefano Berretti. Emovoca: Speech-driven emotional 3d talking heads. *CoRR*, abs/2403.12886, 2024. 2

[55] Dan Oneata, Adriana Stan, and Horia Cucu. Speaker disentanglement in video-to-speech conversion. In *29th European Signal Processing Conference, EUSIPCO 2021, Dublin, Ireland, August 23-27, 2021*, pages 46–50. IEEE, 2021. 3

[56] Ziqiao Peng, Yihao Luo, Yue Shi, Hao Xu, Xiangyu Zhu, Hongyan Liu, Jun He, and Zhaoxin Fan. Selftalk: A self-supervised commutative training diagram to comprehend 3d talking faces. In *Proceedings of the 31st ACM International Conference on Multimedia, MM 2023, Ottawa, ON, Canada, 29 October 2023- 3 November 2023*, pages 5292–5301. ACM, 2023. 2

[57] Ziqiao Peng, Haoyu Wu, Zhenbo Song, Hao Xu, Xiangyu Zhu, Hongyan Liu, Jun He, and Zhaoxin Fan. Emotalk: Speech-driven emotional disentanglement for 3d face animation. *CoRR*, abs/2303.11089, 2023. 1, 2, 3, 4

[58] Hai Xuan Pham, Samuel Cheung, and Vladimir Pavlovic. Speech-driven 3d facial animation with implicit emotional awareness: A deep learning approach. In *2017 IEEE Conference on Computer Vision and Pattern Recognition Workshops, CVPR Workshops 2017, Honolulu, HI, USA, July 21-26, 2017*, pages 2328–2336. IEEE Computer Society, 2017.

[59] Hai Xuan Pham, Yuting Wang, and Vladimir Pavlovic. End-to-end learning for 3d facial animation from raw waveforms of speech. *CoRR*, abs/1710.00920, 2017. 2

[60] K. R. Prajwal, Rudrabha Mukhopadhyay, Vinay P. Namboodiri, and C. V. Jawahar. Learning individual speaking styles for accurate lip to speech synthesis. In *2020 IEEE/CVF Conference on Computer Vision and Pattern Recognition, CVPR 2020, Seattle, WA, USA, June 13-19, 2020*, pages 13793–13802. Computer Vision Foundation / IEEE, 2020. 3

[61] Ofir Press, Noah A. Smith, and Mike Lewis. Train short, test long: Attention with linear biases enables input length extrapolation. In *The Tenth International Conference on Learning Representations, ICLR 2022, Virtual Event, April 25-29, 2022. OpenReview.net*, 2022. 4

[62] Alec Radford, Jong Wook Kim, Chris Hallacy, Aditya Ramesh, Gabriel Goh, Sandhini Agarwal, Girish Sastry, Amanda Askell, Pamela Mishkin, Jack Clark, Gretchen Krueger, and Ilya Sutskever. Learning transferable visual models from natural language supervision. In *Proceedings of the 38th International Conference on Machine Learning, ICML 2021, 18-24 July 2021, Virtual Event*, pages 8748–8763. PMLR, 2021. 3

[63] Alec Radford, Jong Wook Kim, Tao Xu, Greg Brockman, Christine McLeavey, and Ilya Sutskever. Robust speech recognition via large-scale weak supervision. In *International Conference on Machine Learning, ICML 2023, 23-29 July 2023, Honolulu, Hawaii, USA*, pages 28492–28518. PMLR, 2023. 6

[64] George Retsinas, Panagiotis P. Filntasis, Radek Danecek, Victoria F. Abrevaya, Anastasios Roussos, Timo Bolkart, and Petros Maragos. 3d facial expressions through analysis-by-neural-synthesis. In *Proceedings of the IEEE/CVF Conference on Computer Vision and Pattern Recognition (CVPR)*, pages 2490–2501, 2024. 3, 5, 7

[65] Alexander Richard, Michael Zollhöfer, Yandong Wen, Fernando De la Torre, and Yaser Sheikh. Meshtalk: 3d face animation from speech using cross-modality disentanglement. In *2021 IEEE/CVF International Conference on Computer Vision, ICCV 2021, Montreal, QC, Canada, October 10-17, 2021*, pages 1153–1162. IEEE, 2021. 2, 3, 6

[66] Antony W. Rix, John G. Beerends, Michael P. Hollier, and Andries P. Hekstra. Perceptual evaluation of speech quality (pesq)-a new method for speech quality assessment of telephone networks and codecs. In *IEEE International Conference on Acoustics, Speech, and Signal Processing, ICASSP 2001, 7-11 May, 2001, Salt Palace Convention Center, Salt Lake City, Utah, USA, Proceedings*, pages 749–752. IEEE, 2001. 6

[67] Robin Rombach, Andreas Blattmann, Dominik Lorenz, Patrick Esser, and Björn Ommer. High-resolution image synthesis with latent diffusion models. In *IEEE/CVF Conference on Computer Vision and Pattern Recognition, CVPR 2022, New Orleans, LA, USA, June 18-24, 2022*, pages 10674–10685. IEEE, 2022. 2

[68] Soubhik Sanyal, Timo Bolkart, Haiwen Feng, and Michael J. Black. Learning to regress 3d face shape and expression from an image without 3d supervision. In *IEEE Conference on Computer Vision and Pattern Recognition, CVPR 2019, Long Beach, CA, USA, June 16-20, 2019*, pages 7763–7772. Computer Vision Foundation / IEEE, 2019. 5

[69] Stefan Stan, Kazi Injamamul Haque, and Zerrin Yumak. Facediffuser: Speech-driven 3d facial animation synthesis using diffusion. In *Proceedings of the 16th ACM SIGGRAPH Conference on Motion, Interaction and Games*, pages 1–11, 2023. 2, 3, 7

[70] Zhiyao Sun, Tian Lv, Sheng Ye, Matthieu Gaetan Lin, Jenny Sheng, Yu-Hui Wen, Minjing Yu, and Yong-Jin Liu. Diffposetalk: Speech-driven stylistic 3d facial animation and head pose generation via diffusion models. *CoRR*, abs/2310.00434, 2023. 2, 3, 4, 6, 7, 5

[71] Cees H. Taal, Richard C. Hendriks, Richard Heusdens, and Jesper Jensen. An algorithm for intelligibility prediction of time-frequency weighted noisy speech. *IEEE Trans. Speech Audio Process.*, 19(7):2125–2136, 2011. 6

[72] Sarah L. Taylor, Moshe Mahler, Barry-John Theobald, and Iain A. Matthews. Dynamic units of visual speech. In *Proceedings of the 2012 Eurographics/ACM SIGGRAPH Symposium*

on Computer Animation, SCA 2012, Lausanne, Switzerland, 2012, pages 275–284. Eurographics Association, 2012. 2

[73] Sarah L. Taylor, Taehwan Kim, Yisong Yue, Moshe Mahler, James Krahe, Anastasio Garcia Rodriguez, Jessica K. Hodgins, and Iain A. Matthews. A deep learning approach for generalized speech animation. *ACM Trans. Graph.*, 36(4):93:1–93:11, 2017. 2

[74] Guy Tevet, Sigal Raab, Brian Gordon, Yoni Shafir, Daniel Cohen-or, and Amit Haim Bermano. Human motion diffusion model. In *The Eleventh International Conference on Learning Representations*, 2023. 2

[75] Ayush Tewari, Michael Zollhöfer, Hyeongwoo Kim, Pablo Garrido, Florian Bernard, Patrick Pérez, and Christian Theobalt. Mofa: Model-based deep convolutional face autoencoder for unsupervised monocular reconstruction. In *IEEE International Conference on Computer Vision, ICCV 2017, Venice, Italy, October 22-29, 2017*, pages 3735–3744. IEEE Computer Society, 2017. 5

[76] Ayush Tewari, Michael Zollhöfer, Pablo Garrido, Florian Bernard, Hyeongwoo Kim, Patrick Pérez, and Christian Theobalt. Self-supervised multi-level face model learning for monocular reconstruction at over 250 hz. In *2018 IEEE Conference on Computer Vision and Pattern Recognition, CVPR 2018, Salt Lake City, UT, USA, June 18-22, 2018*, pages 2549–2559. Computer Vision Foundation / IEEE Computer Society, 2018.

[77] Ayush Tewari, Florian Bernard, Pablo Garrido, Gaurav Bharaj, Mohamed Elgharib, Hans-Peter Seidel, Patrick Pérez, Michael Zollhöfer, and Christian Theobalt. FML: face model learning from videos. In *IEEE Conference on Computer Vision and Pattern Recognition, CVPR 2019, Long Beach, CA, USA, June 16-20, 2019*, pages 10812–10822. Computer Vision Foundation / IEEE, 2019. 5

[78] Balamurugan Thambiraja, Sadegh Aliakbarian, Darren Cosker, and Justus Thies. 3diface: Diffusion-based speech-driven 3d facial animation and editing, 2023. 2, 3

[79] Balamurugan Thambiraja, Ikhsanul Habibie, Sadegh Aliakbarian, Darren Cosker, Christian Theobalt, and Justus Thies. Imitator: Personalized speech-driven 3d facial animation, 2023. 2, 3, 6

[80] Seyun Um, Jihyun Kim, Jihyun Lee, and Hong-Goo Kang. Facetron: A multi-speaker face-to-speech model based on cross-modal latent representations. In *31st European Signal Processing Conference, EUSIPCO 2023, Helsinki, Finland, September 4-8, 2023*, pages 281–285. IEEE, 2023. 3

[81] Ashish Vaswani, Noam Shazeer, Niki Parmar, Jakob Uszkoreit, Llion Jones, Aidan N Gomez, Łukasz Kaiser, and Illia Polosukhin. Attention is all you need. *Advances in neural information processing systems*, 30, 2017. 2, 4

[82] Thomas Vetter and Volker Blanz. Estimating coloured 3D face models from single images: An example based approach. In *ECCV*, pages 499–513, 1998. 5

[83] Konstantinos Vougioukas, Pingchuan Ma, Stavros Petridis, and Maja Pantic. Video-driven speech reconstruction using generative adversarial networks. In *20th Annual Conference of the International Speech Communication Association, Interspeech 2019, Graz, Austria, September 15-19, 2019*, pages 4125–4129. ISCA, 2019. 3

[84] Kaisiyuan Wang, Qianyi Wu, Linsen Song, Zhuoqian Yang, Wayne Wu, Chen Qian, Ran He, Yu Qiao, and Chen Change Loy. MEAD: A large-scale audio-visual dataset for emotional talking-face generation. In *Computer Vision - ECCV 2020 - 16th European Conference, Glasgow, UK, August 23-28, 2020, Proceedings, Part XXI*, pages 700–717. Springer, 2020. 7

[85] Cheng-hsin Wuu, Ningyuan Zheng, Scott Ardisson, Rohan Bali, Danielle Belko, Eric Brockmeyer, Lucas Evans, Timothy Godisart, Hyowon Ha, Alexander Hypes, Taylor Koska, Steven Krenn, Stephen Lombardi, Xiaomin Luo, Kevyn McPhail, Laura Millerschoen, Michal Perdoch, Mark Pitts, Alexander Richard, Jason M. Saragih, Junko Saragih, Takaaki Shiratori, Tomas Simon, Matt Stewart, Autumn Trimble, Xinshuo Weng, David Whitewolf, Chenglei Wu, Shou-I Yu, and Yaser Sheikh. Multiface: A dataset for neural face rendering, 2022. 3

[86] Jinbo Xing, Menghan Xia, Yuechen Zhang, Xiaodong Cun, Jue Wang, and Tien-Tsin Wong. Codetalker: Speech-driven 3d facial animation with discrete motion prior. pages 12780–12790, 2023. 2, 3, 4, 6

[87] Yuyu Xu, Andrew W. Feng, Stacy Marsella, and Ari Shapiro. A practical and configurable lip sync method for games. In *Motion in Games, MIG '13, Dublin, Ireland, November 6-8, 2013*, pages 131–140. ACM, 2013. 2

[88] Zhihao Xu, Shengjie Gong, Jiapeng Tang, Lingyu Liang, Yining Huang, Haojie Li, and Shuangping Huang. Kmtalk: Speech-driven 3d facial animation with key motion embedding. In *Computer Vision - ECCV 2024 - 18th European Conference, Milan, Italy, September 29-October 4, 2024, Proceedings, Part LVI*, pages 236–253. Springer, 2024. 2

[89] Ravindra Yadav, Ashish Sardana, Vinay P. Namboodiri, and Rajesh M. Hegde. Speech prediction in silent videos using variational autoencoders. In *IEEE International Conference on Acoustics, Speech and Signal Processing, ICASSP 2021, Toronto, ON, Canada, June 6-11, 2021*, pages 7048–7052. IEEE, 2021. 3

[90] Karren D. Yang, Anurag Ranjan, Jen-Hao Rick Chang, Raviteja Vemulapalli, and Oncel Tuzel. Probabilistic speech-driven 3d facial motion synthesis: New benchmarks, methods, and applications. *CoRR*, abs/2311.18168, 2023. 2, 5, 7

[91] Yochai Yemini, Aviv Shamsian, Lior Bracha, Sharon Gannot, and Ethan Fetaya. Lipvoicer: Generating speech from silent videos guided by lip reading. *CoRR*, abs/2306.03258, 2023. 3

[92] Tianke Zhang, Xuangeng Chu, Yunfei Liu, Lijian Lin, Zhen-dong Yang, Zhengzhuo Xu, Chengkun Cao, Fei Yu, Changyin Zhou, Chun Yuan, and Yu Li. Accurate 3d face reconstruction with facial component tokens. In *IEEE/CVF International Conference on Computer Vision, ICCV 2023, Paris, France, October 1-6, 2023*, pages 8999–9008. IEEE, 2023. 3, 5

[93] Qingcheng Zhao, Pengyu Long, Qixuan Zhang, Dafei Qin, Han Liang, Longwen Zhang, Yingliang Zhang, Jingyi Yu, and Lan Xu. Media2face: Co-speech facial animation generation with multi-modality guidance, 2024. 2, 3, 4, 6, 7, 5

[94] Yang Zhou, Zhan Xu, Chris Landreth, Evangelos Kalogerakis, Subhransu Maji, and Karan Singh. Visemenet: Audio-driven

animator-centric speech animation. *ACM Trans. Graph.*, 37(4), 2018. [2](#)

[95] Wojciech Zielenka, Timo Bolkart, and Justus Thies. Towards metrical reconstruction of human faces. In *Computer Vision - ECCV 2022 - 17th European Conference, Tel Aviv, Israel, October 23-27, 2022, Proceedings, Part XIII*, pages 250–269. Springer, 2022. [3](#), [6](#), [2](#), [4](#), [5](#), [7](#)

A. Additional Experiments

A.1. Mesh-to-Speech

Per-Dataset Performance Analysis. The performance of both mesh-to-speech and video-to-speech models varies dramatically depending on the dataset. Datasets with limited number of utterances and vocabulary such as RAVDESS or GRID are less challenging, and the models can regress relatively accurately, sometimes to the point of perfect intelligibility. On the more challenging TCD-TIMIT dataset, which contains more complex vocabulary, words are often missed. However, despite the relatively high word error rate (WER) on TCD-TIMIT, the produced sounds, remain very realistic, given the animation. Please see Tab. 3 for per-dataset breakdown and refer to the supplementary video for an audible comparison.

A.2. Talking Heads

A.2.1. Disentanglement

Ideally, mesh-to-speech should help preserve high-quality lip-sync in the presence of other editing conditions. In other words, the lip-sync should effectively be disentangled from other conditions. To validate this, we evaluate our re-implementations of Media2Face on our test set, passing additional conditioning inputs extracted from emotional images. The conditioning images can be found in Fig. 7. For example results of Media2Face animations, please refer to the supplementary video. The metrics can be found in Tab. 4.

DATASET	Model:	STOI \uparrow	ESTOI \uparrow	PESQ-WB \uparrow	PESQ-NB \uparrow	WER \downarrow
GRID	exp2speech x	0.533	0.290	1.298	1.552	0.553
	face2speech V	0.482	0.211	1.261	1.513	0.783
	mouth2speech $V_{m \in M}$	0.538	0.295	1.288	1.539	0.559
	Choi et al. (finetuned)	0.590	0.371	1.324	1.597	0.428
	Choi et al.	0.426	0.158	1.137	1.345	1.202
RAVDESS	exp2speech x	0.460	0.284	1.159	1.262	0.145
	face2speech V	0.474	0.293	1.164	1.266	0.173
	mouth2speech $V_{m \in M}$	0.510	0.328	1.161	1.262	0.131
	Choi et al. (finetuned)	0.548	0.375	1.174	1.277	0.060
	Choi et al.	0.452	0.245	1.074	1.149	0.774
TCD-TIMIT	exp2speech x	0.409	0.206	1.146	1.249	0.929
	face2speech V	0.368	0.139	1.117	1.228	1.431
	mouth2speech $V_{m \in M}$	0.389	0.174	1.131	1.243	1.070
	Choi et al. (finetuned)	0.436	0.257	1.168	1.293	0.579
	Choi et al.	0.172	0.041	1.103	1.254	0.641
COMBINED	exp2speech x	0.502	0.273	1.257	1.468	0.648
	face2speech V	0.458	0.203	1.225	1.437	0.953
	mouth2speech $V_{m \in M}$	0.506	0.272	1.246	1.457	0.678
	Choi et al. (finetuned)	0.555	0.348	1.281	1.511	0.437
	Choi et al. (orig)	0.376	0.141	1.126	1.313	1.011

Table 3. **Quantitative comparison of mesh-to-speech with silent-video-to-speech.** While Choi et al. outperforms THUNDER in most cases, the performance is comparable. The performance of both methods depends dramatically on the test dataset. Inputs from datasets with limited vocabulary (GRID, RAVDESS) tend to produce lower word error rates than datasets with richer vocabulary (TCD-TIMIT).

Name	LVE \downarrow	LIP CCC \uparrow	LIP PCC \uparrow	DTW \downarrow	S-DIV-L \downarrow
M2F-F* orig.	0.611	0.522	0.617	0.221	0.0956
M2F-F* w/ m2s orig.	0.551	0.558	0.679	0.212	0.027
M2F-F* angry	1.6	0.307	0.526	0.914	0.151
M2F-F* w/ m2s angry	1.46	0.348	0.59	0.741	0.08
M2F-F* calm	0.91	0.369	0.537	0.297	0.103
M2F-F* w/ m2s calm	0.86	0.459	0.638	0.302	0.0289
M2F-F* disgust	0.928	0.314	0.527	0.316	0.0675
M2F-F* w/ m2s disgust	0.874	0.426	0.627	0.305	0.019
M2F-F* fearful	1.01	0.38	0.618	0.315	0.101
M2F-F* w/ m2s fearful	1.03	0.353	0.627	0.303	0.0295
M2F-F* happy	1.31	0.201	0.394	0.484	0.152
M2F-F* w/ m2s happy	1.11	0.3	0.597	0.269	0.047
M2F-F* sad	0.96	0.308	0.531	0.363	0.108
M2F-F* w/ m2s sad	0.815	0.428	0.609	0.282	0.0371
M2F-F surprised	1.04	0.391	0.576	0.494	0.0759
M2F-F w/ m2s surprised	1.06	0.366	0.602	0.362	0.0278

Table 4. **Disentanglement effect.** We feed different input conditions to our versions of Media2Face* models and report the lip-sync metrics for both. *Orig.* denotes an image condition extracted from the video that corresponds to the audio. All other rows are results for denoising with other conditions that come from 7 different emotional images. Media2Face* with THUNDER exhibits superior lip-sync in most cases.

A.2.2. Extended Ablation and Sensitivity Analysis

Tab. 5 shows the complete ablation of all THUNDER components. We give a comprehensive evaluation of our design decisions. (1) The input space for the mesh-to-speech loss, (2) the weight of the mesh-to-speech loss, and (3) the trainability of the input audio encoder.

On mesh-to-speech input space. While all three modalities are comparable, *mouth2s* has scores best on the lip-sync metrics, likely thanks to the localized effect on the mouth. *Exp2s* supervision performs slightly worse on lip-sync but results in higher sample diversity. Finally, applying supervision through the whole face to speech (*face2s*), while achieving comparable lip-sync scores, scores worse on diversity, specifically S-DIV-U.



Figure 7. **Media2Face conditioning images.** These images were used as the conditions for the Media2Face* disentanglement experiment in Tab. 4. The images were selected out from the RAVDESS test set. Top row from left to right: happy, angry, sad, disgusted. Bottom row: fearful, surprised, calm.

On mesh-to-speech strength. Applying mesh-to-speech loss, even weakly, results in improved lip-sync metrics (LVE, CCC, PCC and DTW). The stronger the loss, the more the lip-sync metrics improve. However, increasing weights of the mesh-to-speech loss come at the expense of generation diversity (metrics S-DIV, T-DIV).

On finetuning the audio encoder. Nearly all recent methods finetune the input audio encoder or else they suffer from considerably impaired lip-sync. This results in a certain amount of overfitting to the training subjects' voices, which manifests as lower diversity scores (S-DIV-U) compared to the models with frozen Wav2Vec (THUNDER-F). In essence, the model's with trainable audio encoders become less stochastic and more deterministic. Remarkably, the application of the mesh-to-speech loss alleviates the necessity for finetuning Wav2Vec, producing significantly better lip-sync even without finetuning Wav2Vec (THUNDER-T), dramatically reducing the number of training parameters. Applying mesh-to-speech along with finetuning Wav2Vec results in further improvement of lip-sync metrics.

Please refer to the supplementary video for visual examples of all the phenomena described above.

A.2.3. Perceptual Study

Here we provide the rest of our comprehensive perceptual evaluation of THUNDER. We run a perceptual study on Amazon Mechanical Turk. The participants are shown two videos side-by-side. One corresponding to THUNDER and one to a baseline. The left-right order is randomized. The participants must finish watching both videos before being allowed to rate the videos on a five-point Likert scale (strong

preference for left, weak preference for left, indifference, weak preference for right and strong preference for right). We ask the participants to rate three aspects of the animation - lip-sync, dynamism and realism. The exact task description can be seen in the study template in Fig. 14. The participants are shown 20 comparisons, generated from test audios, which were randomly selected from the RAVDESS and TCD-TIMIT test sets. In addition to that, we repeat the first 4 comparisons at the end of the study and discard the first 4 responses. This gives the participants a few examples such that they can adjust to the task. Additionally, we include 4 catch trials, where one animation is selected from Ground Truth and the other animation is clearly wrong. We discard the participants that are wrong on more than one catch trial. The complete results of the perceptual study for THUNDER for lip-sync, dynamism and realism can be found in Figures 8, 9 and 10 respectively. The results for THUNDER-T are given in Figures 11, 12 and 13. The results validate our qualitative and quantitative findings - THUNDER models exhibit better lip-sync, realism and dynamism when compared to baselines.

A.2.4. Generalization to other datasets

To verify whether the performance of THUNDER and mesh-to-speech translates to other types of data, we run additional experiments on TFHP (the DiffPoseTalk dataset [70]). TFHP was reconstructed from YouTube videos. The dataset contains unscripted audios, longer sequences, and the reconstructions were obtained using MICA [95] and SPECTRE [28] and look qualitatively very different compared to our EMICA reconstructions. Can THUNDER work also in this setting?

We train both mesh-to-speech and THUNDER-T on

Name	LVE ↓	L-CCC ↑	L-PCC ↑	DTW ↓	S-DIV-U ↑	T-DIV-U ↑	S-DIV-L ↓	T-DIV-L ↑	FDD-U ↓	FDD-L ↓
THUNDER w/o m2s	0.879	0.359	0.568	0.329	0.0419	0.044	0.21	0.254	<i>0.0118</i>	0.0932
THUNDER w/ face2s	<i>0.804</i>	0.411	0.633	0.285	0.0297	<i>0.0409</i>	0.128	0.237	0.0117	<i>0.0827</i>
THUNDER w/ exp2s	0.83	0.362	0.63	0.296	<i>0.0404</i>	0.0398	0.176	0.228	0.0125	0.0939
THUNDER w/ mouth2s	0.802	0.426	0.639	0.29	0.0322	0.04	<i>0.134</i>	<i>0.241</i>	0.0122	0.0806
THUNDER-F w/o m2s	0.879	0.359	0.568	0.329	<i>0.0419</i>	<i>0.044</i>	0.21	0.254	0.0118	0.0932
THUNDER-F $w_{m2s} = 0.1$	0.887	<i>0.375</i>	<i>0.599</i>	0.309	0.0422	0.0445	0.211	0.258	0.0128	0.0936
THUNDER-F $w_{m2s} = 0.5$	<i>0.805</i>	0.342	0.574	<i>0.294</i>	0.0387	0.0383	0.164	0.225	0.0131	0.103
THUNDER-F $w_{m2s} = 1.0$	0.802	0.426	0.639	0.29	0.0322	0.04	0.134	0.241	<i>0.0122</i>	0.0806
THUNDER-F $w_{m2s} = 5.0$	0.858	0.32	0.572	0.313	0.0257	0.0364	0.159	0.23	0.0143	0.105
THUNDER-F $w_{m2s} = 10.0$	0.886	0.311	0.585	0.31	0.021	0.035	<i>0.146</i>	0.219	0.0155	0.105
THUNDER-T w/o m2s	0.723	0.428	0.623	0.266	0.02	<i>0.0411</i>	<i>0.0656</i>	<i>0.216</i>	0.0118	0.0811
THUNDER-T $w_{m2s} = 0.1$	0.79	0.417	0.63	0.252	0.0279	0.0431	0.0964	0.221	0.0117	0.0729
THUNDER-T $w_{m2s} = 0.5$	0.693	<i>0.435</i>	<i>0.641</i>	0.263	<i>0.0221</i>	0.0391	0.0662	0.201	0.0118	<i>0.0782</i>
THUNDER-T $w_{m2s} = 1.0$	<i>0.709</i>	0.445	0.66	<i>0.256</i>	0.021	0.039	<i>0.0669</i>	0.202	<i>0.0118</i>	<i>0.0788</i>
THUNDER-T $w_{m2s} = 5.0$	0.844	0.343	0.614	0.262	0.0213	0.0351	0.0997	0.203	0.0139	0.0908
THUNDER-T $w_{m2s} = 10.0$	0.737	0.408	0.621	0.301	0.0207	0.0344	0.0486	0.199	0.0147	0.089

Table 5. Ablation study and sensitivity analysis. Here we analyze the effect of the mesh-to-speech loss on the talking head avatar training. The top section compares models supervised with mouth-mesh-to-speech (mouth2s), full-mesh-to-speech (face2s) and flame-to-speech (exp2s). While it is already present in the main paper text, we include it here for completeness. The mid and bottom sections analyze the effect of weight w_{mts} , with either frozen (-F) or trainable (-T) Wav2Vec2. THUNDER-T models exhibit superior lip-sync performance but it comes at the expense of reduced diversity. Furthermore, for both THUNDER-F and THUNDER-T models, increasing w_{mts} , while beneficial for lip animation quality, comes at an increasing expense of diversity. Please refer to the Sup. Video for qualitative comparison.

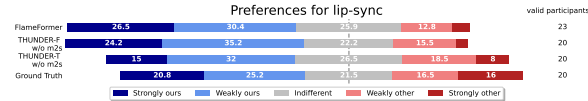


Figure 8. **THUNDER-F perceptual study - lip-sync.** The results of THUNDER-F against other methods. We compare THUNDER-F against methods with both trainable audio encoder (FlameFormer-T, THUNDER-T w/o mesh-to-speech) and frozen encoders (FlameFormer-F, THUNDER-F w/o mesh-to-speech). THUNDER-F outperforms other methods on lip-sync, including those with the trainable audio-encoder (denoted -T).

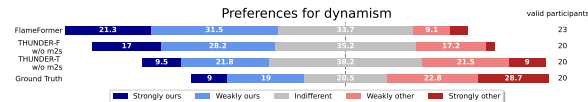


Figure 9. **THUNDER-F perceptual study - dynamism** The participants found THUNDER-F considerably more dynamic than the deterministic FlameFormer and also more dynamic than THUNDER-F w/o mesh-to-speech. However, ground truth is still rated more dynamic.

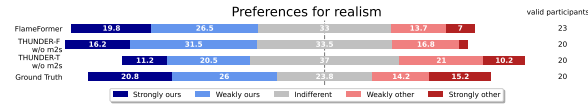


Figure 10. **THUNDER-F perceptual study - realism** The participants found THUNDER-F considerably more dynamic than the deterministic FlameFormer and also more dynamic than THUNDER-F w/o mesh-to-speech. THUNDER-T w/o mesh-to-speech is rated about as realistic as THUNDER. Remarkably, the participants have preferred THUNDER’s generation over ground truth in terms of realism..

TFHP, along with training DiffPoseTalk with the official DiffPoseTalk codebase. Please note, that in order to equalize the input conditions, we trained DiffPoseTalk without identity conditioning. During evaluation, we do not use the style-condition but evaluate using the audio condition only (for both THUNDER models and DiffPoseTalk). The results are reported in Tab. 6.

A.2.5. Comparison to other methods.

Comparing different speech-driven animation methods is a difficult task, especially if trained on a different dataset

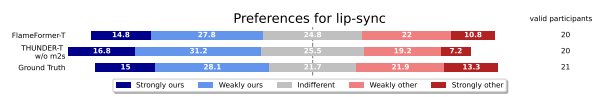


Figure 11. **THUNDER-T complete perceptual study.** The results of THUNDER-T against other methods. THUNDER-T outperforms its counterpart with mesh-to-speech and the deterministic FlameFormer on lip-sync quality. Additionally, the participants have a slight preference for THUNDER-T over ground truth. This suggests, that while THUNDER-T exhibits a degree of dynamism, the GT potential has not yet been fully exhausted.

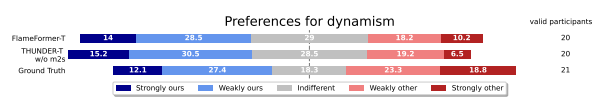


Figure 12. **THUNDER-T perceptual study - dynamism.** The participants rate THUNDER-T to be more dynamic than THUNDER-T without mesh-to-speech and also more dynamic than FlameFormer-T, THUNDER-T w/o mesh-to-speech and even Ground Truth. This suggest that THUNDER-T’s realism exhausted the realism of the dataset.



Figure 13. **THUNDER-T perceptual study - realism.** The participants prefer the degree of realism of THUNDER-T’s outputs over FlameFormer-T

and especially if the data was acquired in different ways (4D scans, pseudo-GT of different reconstruction methods, etc.). Having a fair apples-to-apples comparisons stemming from measurements done against the (pseudo-) ground truth is therefore difficult. Regardless, for the sake of completeness, we compare THUNDER to the official releases of recent methods that were also trained on pseudo-GT, namely EMOTE [17] (a deterministic SOTA) and DiffPoseTalk [70] (stochastic SOTA). EMOTE is a FaceFormer-inspired architecture with additional input conditions for emotions and intensity, trained with a content-emotion disentanglement mechanism. It was trained on pseudo-GT reconstructions of MEAD. The pGT was acquired with the same INFERNO

Name	LVE ↓	L-CCC ↑	L-PCC ↑	DTW ↓	S-DIV-U ↑	T-DIV-U ↑	S-DIV-L ↓	T-DIV-L ↑	T-FDD-U ↓
DiffPoseTalk (w/o style cond.)	1.24	0.341	0.508	0.25	0.0388	0.0395	0.235	0.318	0.0111
THUNDER-T w/o m2s	1.1	0.332	0.518	0.226	0.0208	0.0293	0.122	0.277	0.0068
THUNDER-T	1.09	0.351	0.545	0.214	0.0255	0.0322	0.103	0.265	0.00777

Table 6. **Experiment on TFHP.** We compare THUNDER-T, THUNDER w/o mesh-to-speech and DiffPoseTalk (all trained on TFHP). Similarly to our other experiments, THUNDER-T results in superior lip-sync metrics, while trading off upper-face diversity.

Decide which video has better facial animations

In this task you are presented with two videos of virtual characters animated by two different methods. Their facial motions and lip-sync are generated from the same audio.

Both videos have sound, please listen to them!

You will be asked to select your preference between the two videos according to two different criteria:

1. Which video has better synchronization of the lips with the speech?
 Please select the animations have more plausible lip-sync. Please pay attention to:
 (1) Focus on the correct articulation of the individual syllables.
 (2) Is the mouth opening and closing in sync with the speech?
 (3) Is the mouth closed upon pronunciation of sounds like "m", "b" and "p"?
 Please factor all of the above into your answer.

2. Which video has more lively facial expressions?
 Please select the video where the overall facial motion looks more lively and dynamic.

3. Which video has animations that are more realistic?
 Please select the video where the animation is more realistic. Are there any uncanny effects such as unrealistic or over-exaggerated expressions, lip penetration or face twists?

Possible answers:
 Choose your preference on the scale from left to right, where the leftmost answer means strong preference for the video A, and the rightmost answer means strong preference for the video B, and the middle radio button means no preference.

Please press play in order to start the videos. **You need to watch and listen both videos at least once to be able to answer.**

video A



video B



video A

video B

1. Which video has better lip-synchronization with the spoken audio?

strong preference for video A	weak preference for video A	equally preferred	weak preference for video B	strong preference for video B
<input type="radio"/>	<input type="radio"/>	<input type="radio"/>	<input type="radio"/>	<input type="radio"/>

2. Which video has more lively facial expressions?

strong preference for video A	weak preference for video A	equally preferred	weak preference for video B	strong preference for video B
<input type="radio"/>	<input type="radio"/>	<input type="radio"/>	<input type="radio"/>	<input type="radio"/>

3. Which video is more realistic?

strong preference for video A	weak preference for video A	equally preferred	weak preference for video B	strong preference for video B
<input type="radio"/>	<input type="radio"/>	<input type="radio"/>	<input type="radio"/>	<input type="radio"/>

To proceed, you must select an answer to all questions!

Submit

Figure 14. The perceptual study web template.

tracker, making the resulting metrics comparable. The macro-architecture of DiffPoseTalk’s diffusion is very similar to THUNDER and apart from the additional style conditioning input, it differs only in small details (such as noise schedule, number of denoising steps, etc.). The most important difference is that it was trained on a different dataset, and the re-

constructions were produced by a combination of SPECTRE [28] and MICA [95] and hence look qualitatively very different. As such, the DiffPoseTalk metrics likely dominated by the qualitative difference, and are only listed for completeness. Please note that for this experiment, DiffPoseTalk was run without the style condition (to match the setting of

Name	LVE \downarrow	L-CCC \uparrow	L-PCC \uparrow	DTW \downarrow	S-DIV-U \uparrow	T-DIV-U \uparrow	S-DIV-L \downarrow	T-DIV-L \uparrow	FDD-U \downarrow	FDD-L \downarrow
FlameFormer*	0.809	0.368	0.57	0.291	0.0271	0.0372	0.132	0.239	0.0117	0.0909
EMOTE	1.06	0.221	0.442	0.466	0.0563	0.0401	0.248	0.24	0.0141	0.104
DiffPoseTalk	1.15	0.255	0.38	0.316	0.0345	0.0479	0.226	0.308	0.0141	0.102
THUNDER w/o m2s	0.879	0.359	0.568	0.329	0.0419	0.044	0.21	0.254	0.0118	0.0932
THUNDER	0.802	0.426	0.639	0.29	0.0322	0.04	0.134	0.241	0.0122	0.0806

Table 7. **Quantitative comparison of THUNDER with other speech-driven avatar methods.** Asterisk* indicates we have re-implemented the baseline and trained it on our dataset. (1) *On lip-sync.* THUNDER outperforms all baselines on lip-sync metrics (LVE, CCC, PCC, DTW). (2) *On expression diversity.* DiffPoseTalk exhibits higher temporal face diversity T-DIV-U and L-DIV-U, likely due to the training data reconstructed from videos in-the-wild, which contains more dynamic motions than our in-the-lab reconstructions. EMOTE exhibits high sample upper face diversity S-DIV-U and expression diversity S-DIV-EXP which is due to the random sampling of speaking/emotion/intensity styles, which while high, may not be fitting to the particular input audio. THUNDER w/o m2s and THUNDER follow next in S-DIV-U. DiffPoseTalk (the official model) performs comparatively low on lip-sync and well on both temporal and sample diversity, but the result is likely skewed by the fact that it was trained on different dataset with different types of reconstruction.

THUNDER). Finally, we include a FlameFormer trained on our data, and THUNDER trained without mesh-to-speech. The results are reported in Tab. 7.

A.2.6. Qualitative Results

Diversity Input speech may originate from many different expression and even emotions. A well-trained stochastic model should be able to account for that and generate multiple plausible animations, possibly with different facial expressions. Fig. 15 demonstrates THUNDER’s ability to do so.

Supplementary Video. Our video contains exhaustive set of results which demonstrate the benefits of mesh-to-speech and analysis-by-audio-synthesis. The reader is encouraged to watch the video for our qualitative evaluation.

B. Architecture of Baselines

Fig. 16 shows the architecture of the baselines we reimplemented in this paper.

Media2Face. Our reimplementation of Media2Face is built on our diffusion architecture. In training, we provide additional input of ImageBind[30] features extracted from images of the corresponding videos of the training set. Like the audio condition, this condition is dropped 20% of the time.

DiffPoseTalk. Our reimplementation of DiffPoseTalk is also built on our diffusion architecture. It is trained in two stages. In the first stage we train the contrastive style encoder as proposed by the authors [70]. In training of DiffPoseTalk, we provide the additional style feature on the input. The style feature is extracted from the GT animation sequence. Like the audio condition, the style condition is dropped 20% of the time.

FlameFormer. Our FlameFormer architecture is based on FaceFormer. Like FaceFormer, FlameFormer is a transformer-based deterministic speech-driven animation network that takes addition categorical style condition on the input. Instead of predicting the full vertex space like the original FaceFormer does, FlameFormer predicts FLAME 3DMM coefficients x . Additionally, instead of using

the autoregressive loop with a transformer decoder, FlameFormer’s decoder is a transformer encoder, which eliminates the need for the autoregressive formulation. This does not degrade performance and makes the model more efficient, as was already shown by Danček et al. [17], which have proposed the FlameFormer baseline in their paper. Furthermore, we extend FlameFormer’s conditioning inputs - the subject identity (one-hot vector) is complemented with a one-hot vector for 8 basic emotions and three intensities.

C. Data acquisition

In this section we describe the rationale behind our choice of methodology to reconstruct the 3D faces from videos.

C.1. Choice of methodology

Acquiring high quality 4D scans of sufficient scale and richness is costly, time-consuming and requires specialized hardware. Hence, recent speech-driven animation works [17, 70, 90, 93] have turned to pseudo-GT recovered from videos. This choice comes with an important decision - which face reconstruction methodolgy to use. There are several options but two of the most viable options are:

1) *Optimization-based 3DDM fitting* with analysis-by-image-synthesis [5, 6, 82]. While this options is viable and would produce good results, this optimization-based process is rather inefficient when deployed to many hours of video.

2) *Off-the-shelf face 3DMM regressors.* Due to the computational intensity of optimization-based fitting and thanks to the recent advance in deep-learning based in-the-wild face reconstruction methods [16, 20, 27, 28, 64, 68, 75–77, 92, 95]. While this is still an active area of research, and no method produces results that could be considered as accurate as 4D scans, recent years have brought enough advancement so that they can be employed for speech-driven animation dataset construction.

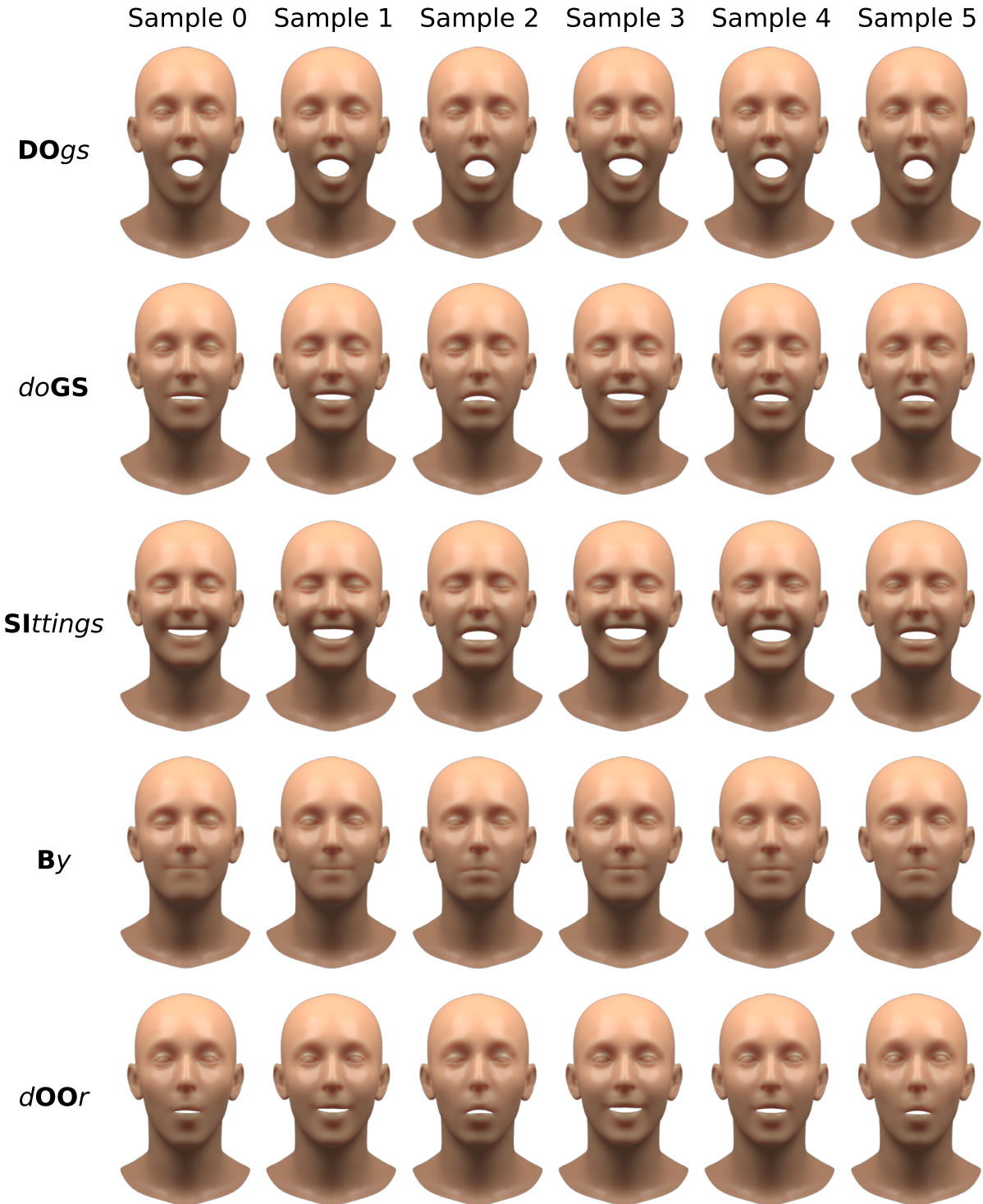


Figure 15. **Diversity of outputs.** THUNDER is capable of generating multiple plausible animations per audio. Each row of this figure contains 6 different generations of the same frame denoised from different initial noise samples (the audio condition remains the same for all).

C.2. Discussion of FLAME regressors

Since THUNDER utilizes FLAME [48], our discussion will focus on FLAME regressors (trackers) only. There are sev-

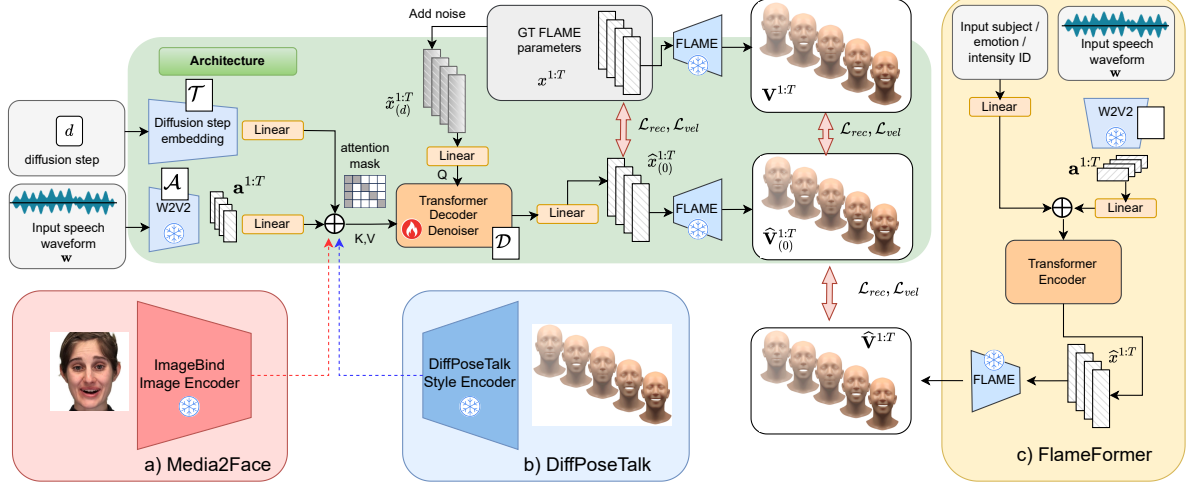


Figure 16. **Architecture of re-implemented baselines.** (a) Our version of Media2Face [93] utilized the same architecture as THUNDER but takes an extra ImageBind feature on the input. (c) Our re-implementation of DiffPoseTalk [70] is also based on THUNDER and takes an extra style feature from a pretrained style encoder. (c) FlameFormer is an adapted FaceFormer [25]. FlameFormer predicts FLAME expression instead of full vertex space. Furthermore, FlameFormer adapts a non-autoregressive BERT-like prediction mechanism (akin to EMOTE [17]).

eral systems that have been used for talking head avatar research. No tracker Each tracker produces different kinds of errors but they were used in prior works on 3D talking head avatars. Here we briefly discuss some of the most applicable candidates:

- DECA [27] is the first FLAME-based regressor trained with the self-supervised "analysis-by-image-synthesis" loop. However, it is limited in terms of richness of expressions and quality of lip animations.
- EMOCA [16] is a follow-up of DECA, capable of reconstruct rich emotions thanks to its emotion-consistency loss. However it can exaggerate expressions and the lip-sync is not good enough.
- SPECTRE [28] applies a paradigm similar to EMOCA but leverages a lip-reading consistency loss instead. It produces good lip-readable animations, but unfortunately often exaggerates, is not capable of reconstructing rich emotional expressions and the disentanglement between expression and identity is rather poor.
- EMICA [18] is a combination of the DECA, EMOCA and SPECTRE putting together the benefits of them all to achieve high quality emotions and lip-sync. Additionally, EMICA makes use of MICA [95] for a consistent identity prediction. The system is trained jointly and publicly available.
- SMIRK [64] SMIRK is a recent reconstruction method which uses a neural renderer and in-the-loop neural data augmentation to produce high quality reconstructions.

C.3. Previous works

As a result of the tremendous progress of in-the-wild face reconstruction, some of the recent SOTA speech-driven animation have already turned to pseudo-GT as the primary source of data.

- EMOTE [17] employed the EMICA model to reconstruct the MEAD [84] dataset.
- Yang et al. [90] utilized both DECA and SPECTRE to reconstruct LRS3 [1].
- DiffPoseTalk employed MICA and SPECTRE separately and then combined the shape predictions of MICA and expression predictions of SPECTRE to reconstruct TFHP.
- EMOCA exaggerates expressions.
- DECA's lip-sync and expressions are very limited.
- We opt for EMICA as it provides a good compromise - rich emotions, good lip animations, consistent shape identity and temporal consistency. That said, it is not artifact-free (mouth wide open correlates with raised eyebrows, etc.) but it is sufficient to use for our research.

Following EMOTE, we opt to use EMICA in this work as well.